ORNL/TM-5862
Dist. Category UC-79,
-79e, -79p

Contract No. W-7405-eng-26

Engineering Technology Division

LOCAL SODIUM BOILING IN A PARTIALLY BLOCKED SIMULATED LMFBR SUBASSEMBLY (THORS BUNDLE 3B)

N. Hanus M. H. Fontana
P. A. Gnadt J. L. Wantland

Manuscript Completed - May 4, 1977
Date Published — June 1977

NOTICE: This document contains information of a preliminary nature. It is subject to revision or correction and therefore does not represent a final report.

Prepared by
OAK RIDGE NATIONAL LABORATORY
Oak Ridge, Tennessee 37830
operated by
UNION CARBIDE CORPORATION
for the
ENERGY RESEARCH AND DEVELOPMENT ADMINISTRATION

DISCLAIMER

CONTENTS

LOCAL SODIUM BOILING IN A PARTIALLY BLOCKED SIMULATED LMFBR SUBASSEMBLY (THORS BUNDLE 3B)

N. Hanus M. H. Fontana
P. A. Gnadt J. L. Wantland

ABSTRACT

Experimental data from local sodium boiling tests with and without argon gas injection have been analyzed. The experiments were conducted with a 19-rod simulated LMFBR subassembly having the six central flow channels (12% of flow area) blocked in the heated section of the bundle. The data analysis shows that, without gas injection, local boiling in the blockage wake does not radially propagate to the surrounding free stream during two quasi-steady-state boiling periods of 13 and 27 sec. However, in tests with argon gas void fractions of 0.001 and 0.004, there is some evidence that the local boiling zone did spread but did not encompass the entire bundle cross section. An idealized extrapolation to full-size LMFBR subassemblies shows that the results with the 19-rod bundle are conservative.

Analysis of data from nonboiling tests with gas injection shows that for void fractions between 0.00009 and 0.00354, the maximum temperature increase in the blockage wake due to gas injection is 40°C (70°F).

Key words: sodium, boiling, LMFBR, safety fuel pins, thermal-hydraulic experiment, electrical heaters, data analysis, heat transfer analysis, fission-gas release, flow blockage, ex-reactor experiment.

INTRODUCTION

An understanding of the effects of in-core blockages is of paramount importance in LMFBR safety. These blockages can result from the accumulation of debris circulated in the primary sodium or from swelling or bowing of the fuel pins. High temperatures downstream from a blockage could, under certain adverse conditions, lead to localized boiling. Tests were conducted in the Thermal-Hydraulic Out-of-Reactor Safety (THORS) facility [formerly the Fuel Failure Mockup (FFM)] in an attempt to determine (1) if local boiling in a blockage wake spreads radially or axially during quasi-steady-state conditions of flow and power (unstable boiling) and (2) if dryout occurs in the local boiling zone in the wake during prolonged periods of constant flow and power.

The subsequent analysis addresses these two phenomena by examining the experimental results of boiling downstream of a 6-channel central non-heat-generating blockage in a 19-pin electrically heated simulated LMFBR subassembly. Approximately 12% of the total flow area in the rod bundle was blocked. In some of these tests, argon gas was injected at the entrance of the bundle in an attempt to simulate fission-gas release from a reactor fuel rod. The extrapolation of the 19-rod (bundle 3B) experimental results to 217-pin LMFBR subassemblies is discussed, with particular emphasis on the differences between the test bundle and an LMFBR fuel subassembly. Neither bundle 3B nor the THORS facility was designed for sustained sodium boiling. (The facility was later modified for modest boiling experiments.)

This analysis is divided into three parts, corresponding to the types of tests conducted: (1) boiling at constant flow and constant power without gas injection, (2) boiling at constant flow and constant power with gas injection, (3) single-phase tests at various combinations of constant flow, power, and gas-injection rates. The single-phase tests, although not directly pertaining to the main objectives of the bundle 3B test program, were added in order to determine the temperature increase downstream of the blockage as a function of flow, heater power, inert-gas void fraction, and time after termination of gas injection.

DESCRIPTION OF TEST FACILITY

Thermal-Hydraulic Out-of-Reactor Safety (THORS) Facility

The THORS facility is a high-temperature sodium facility in which test bundles that duplicate segments of LMFBR core subassemblies are subjected to thermal-hydraulic testing during normal and abnormal reactor conditions. The LMFBR fuel pins are simulated by electric cartridge heaters that have the same outside diameter as a reactor fuel pin; each fuel pin simulator can contain up to four grounded thermocouple junctions attached to the inner surface of the cladding. Helically wrapped wirelike spacers containing either grounded or ungrounded thermocouple junctions separate the fuel pin simulators in the assemblies. These spacers have the same outside diameter and are installed at the same pitch as those used in the Fast Flux Test Facility (FFTF) and in the Clinch River Breeder Reactor (CRBR).

A simplified flow diagram of the THORS facility as it existed for the tests described is shown in Fig. 1. A variable-speed pump and throttle valves are used to vary sodium flow through the test section, and a 440-kVA transformer bank provides electrical power to the simulated fuel pins. Power to the individual pins may be varied from zero to 24.5 kW per element. A heat exchanger rated at 420 kW with an average sodium temperature of 538°C (1000°F) removes the heat that enters the system through the fuel pin simulators in the test bundle. The bundles may be installed through either the top or the bottom of the test-section housing. Design details of the individual components are given in Ref. 1.

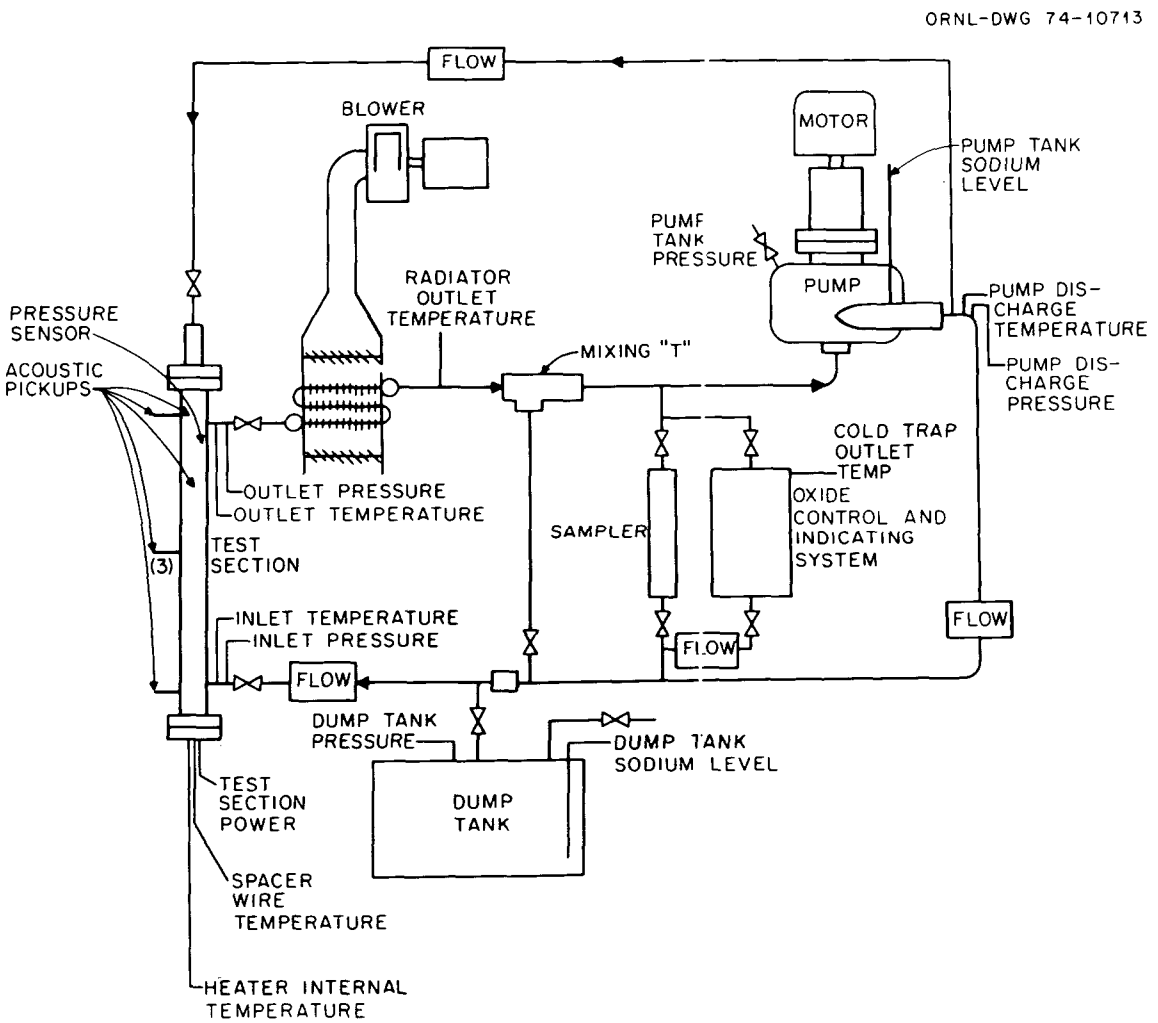

Fig. 1. LMFBR THORS facility flow diagram.

Construction of the THORS facility was completed in December 1970, and five 19-rod bundles of different designs have been tested in the facility. Bundles 1A and 1B were unblocked bundles in a scalloped duct.[2] Bundle 2, which was enclosed in a hexagonal duct, was originally designed to obtain thermal-hydraulic data (without a blockage); in this configuration it was referred to as bundle 2A.[3] After completion of the test program with the bundle in this configuration, the bundle was still viable. The bundle was then inverted in the test section and operated with blockage plates of various sizes installed at the inlet of the bundle. In this configuration, it was referred to as bundle 2B.[4] Bundle 3A[5] was in a scalloped duct with dummy wire-wrap segments on the dummy edge rods and contained a six-channel central blockage. Bundle 3B, the subject of this report, was identical to bundle 3A but had a different test program. Bundle 5, located in a hexagonal duct with half-size [0.71-mm (0.028-in.)] wire spacers between the heaters and the duct wall, was designed for operation in four configurations. Bundles 5A[6] and 5B[7] contained a blockage along one of the hexagonal sides that blocked one-third of the flow area. Bundle 5C[7] was run with the blockage plate removed. Bundle 5D,[8] which was run with the blockage plate removed, was the first bundle operated at the THORS facility at temperatures high enough to produce sodium boiling.

Sodium has been circulated in the THORS loop piping at temperatures as high as 650°C (1200°F); however, sodium temperatures in the test section have reached temperatures of up to 980°C (1800°F). Power levels have been as high as 36.0 kW/m (11.8 kW/ft) per rod in the simulated fuel elements at a maximum test-section flow of 3.4 liters/sec (54 gpm).

Fuel Pin Simulators

The heaters used to simulate the individual fuel rods were manufactured by the Watlow Electric Manufacturing Company, St. Louis, Mo., in accordance with specifications given in Ref. 9. Figure 2 shows the important characteristics of the heaters used in bundle 3B. Voltage is applied to the heating element through the copper lead at the open end of the heater and the electric circuit is completed at the opposite end, where the element is grounded through an end plug to the sodium. Heat is generated over a desired length in the Nichrome V winding. The core inside the winding and

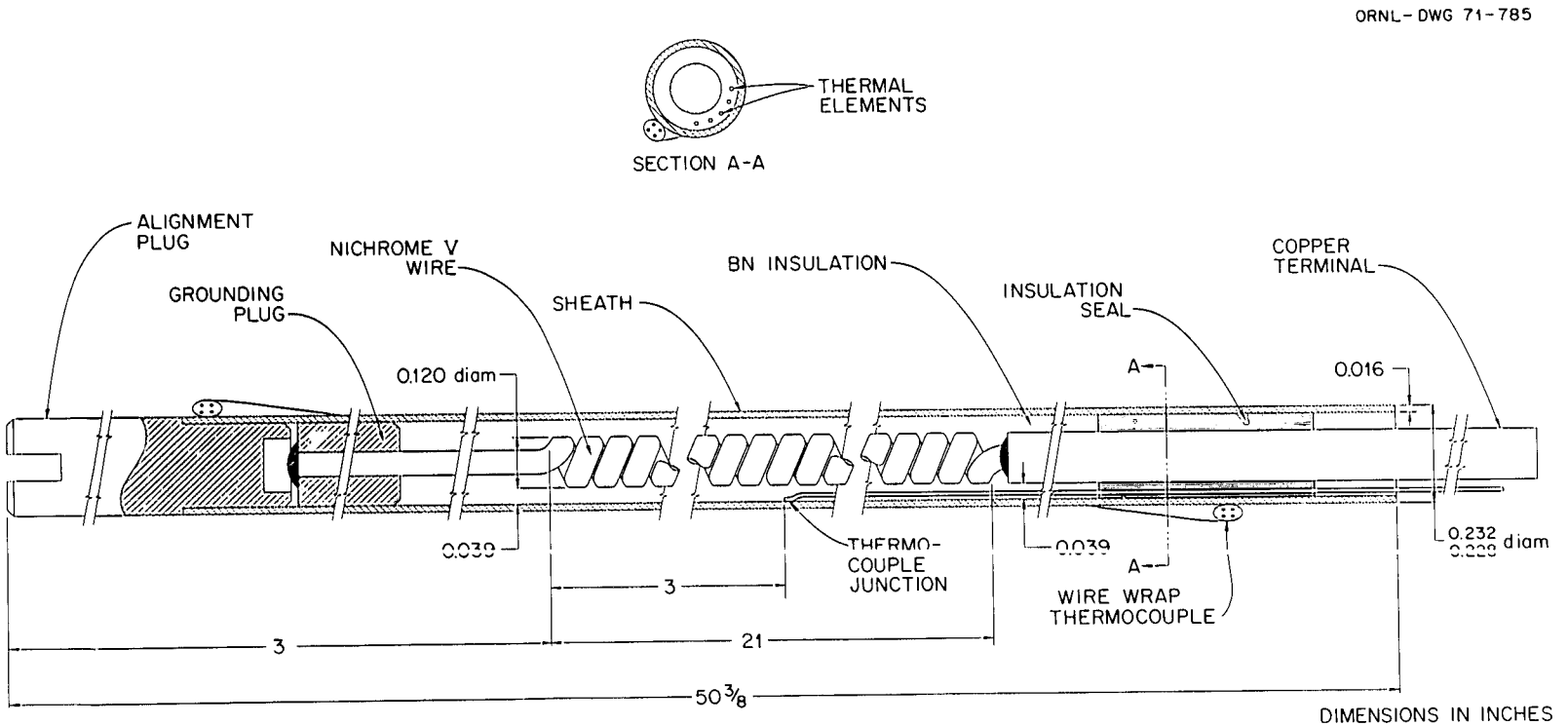

Fig. 2. Heater for bundles 3A and 3B (1 in. = 25.4 mm).

the insulation between the winding and the type 316 stainless steel sheath are of compacted boron nitride. These heaters are described further in Refs. 10 and 11.

Test Section and Rod Bundle 3B

Bundle 3A,[5] which was used for steady-state, nonboiling experiments without gas injection, is shown in Fig. 3. Two additional features (not shown in the figure) were incorporated for the bundle 3B tests. An attemperator, shown in Fig. 4, injected "cold" sodium (at the bundle inlet temperature) into the relatively hot sodium exiting from the bundle to protect the test-section exit piping from excessive temperatures. Also, a section of removable insulation was added to the test-section housing in an effort to allow additional cooling of the sodium containment system. An argon gas injection system (Fig. 5) made it possible to inject argon gas into the sodium stream at the test-section inlet. Analogous tests were made with and without gas injection. These additional features are described in detail in Ref. 12.

Bundle 3B consists of 19 electrically heated pins in a scalloped duct. The pins are 5.84 mm (0.230 in.) in diameter and are spaced by 1.42-mm-diam (0.056-in.) wires wrapped on a 305-mm (12.0-in.) helical pitch. The heated length is 530 mm (21.0 in.). A thermocouple rake assembly, which was also used as the attemperator, is installed at the upper end of the test section to measure bundle exit temperatures. The six central flow channels are blocked by a non-heat-generating stainless steel blockage plate. The blockage plate is 6 mm (1/4 in.) long and is brazed to the central rod 380 mm (15 in.) downstream from the start of the heated section. All bundle 3B heaters have a rated power of 33 kW/m (10 kW/ft); they were not designed for boiling conditions.

Figure 6 is a photograph of the end of bundle 3B taken prior to its installation in the facility. The partially assembled bundle is shown in Fig. 7. Figure 8 shows the thermocouple rake—attemperator assembly near the end of the bundle prior to installation in the facility. Figure 9 is a photograph of the power lead end of the bundle, showing the instrumentation connectors that were used to connect the bundle to the facility wiring.

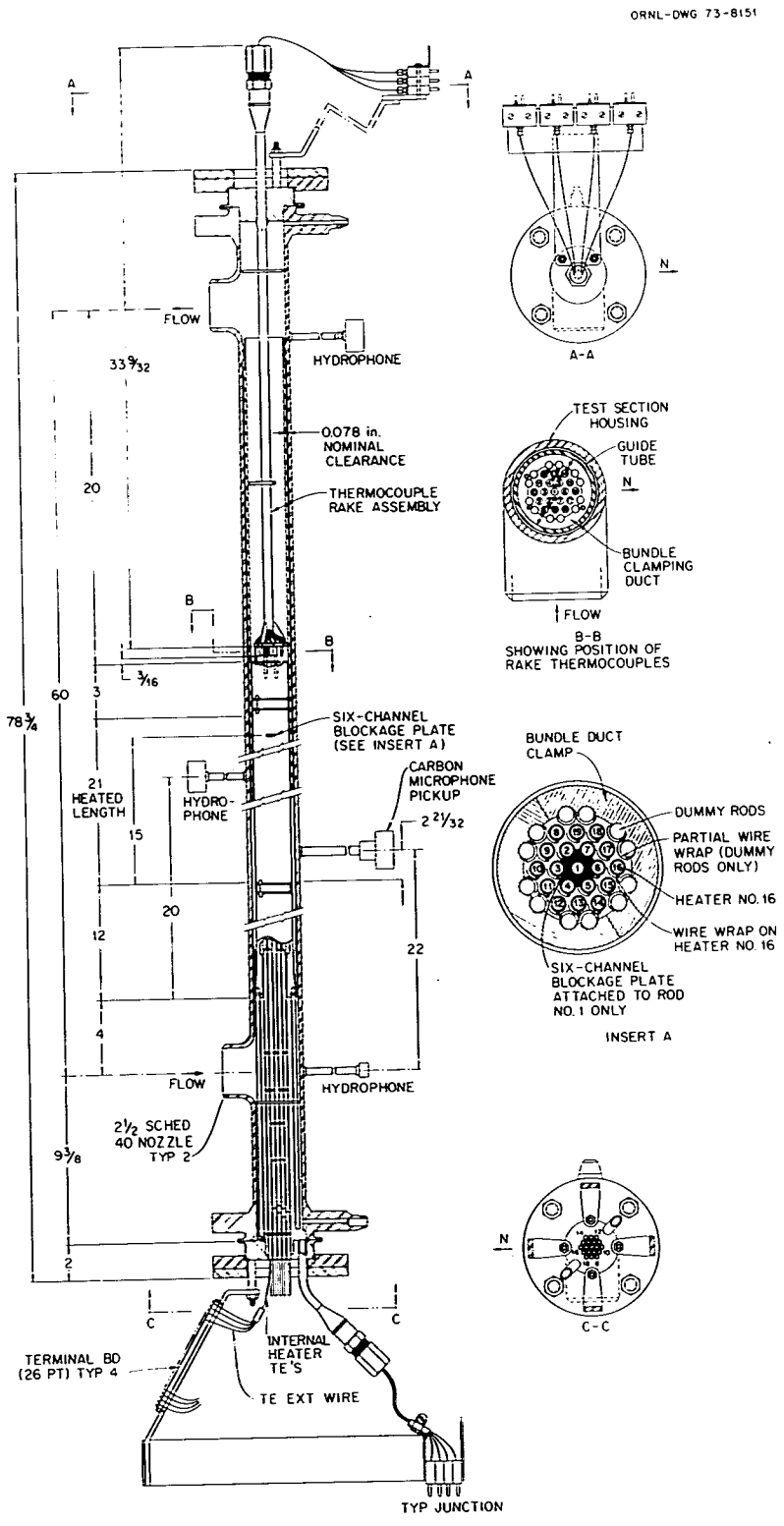

Fig. 3. Test section for bundles 3A and 3B; 19 rods in a scalloped duct with partial wire wraps attached to dummy rods (1 in. = 25.4 mm).

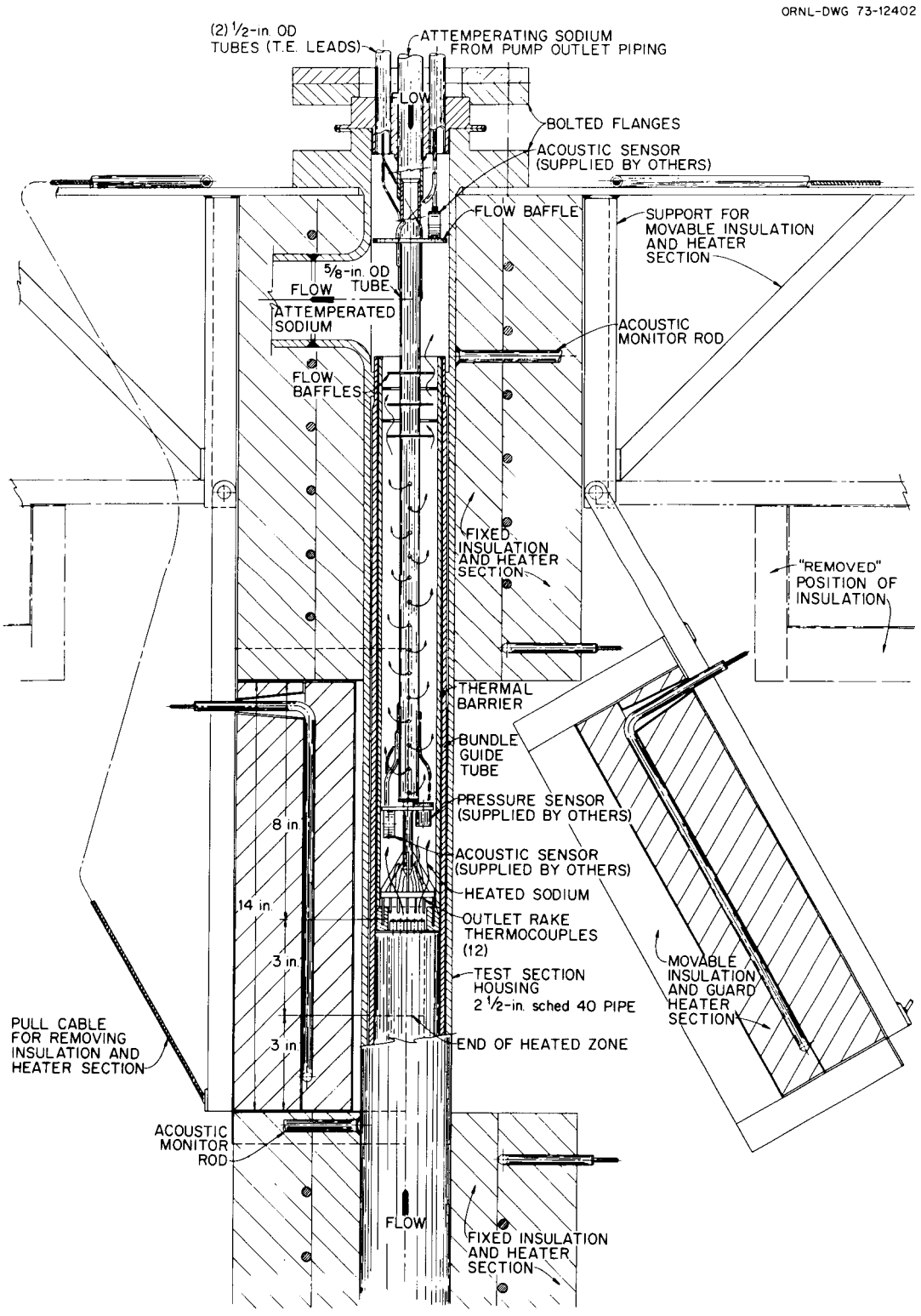

Fig. 4. Modified test-section housing (with attemperator) for bundle 3B (1 in. = 25.4 mm).

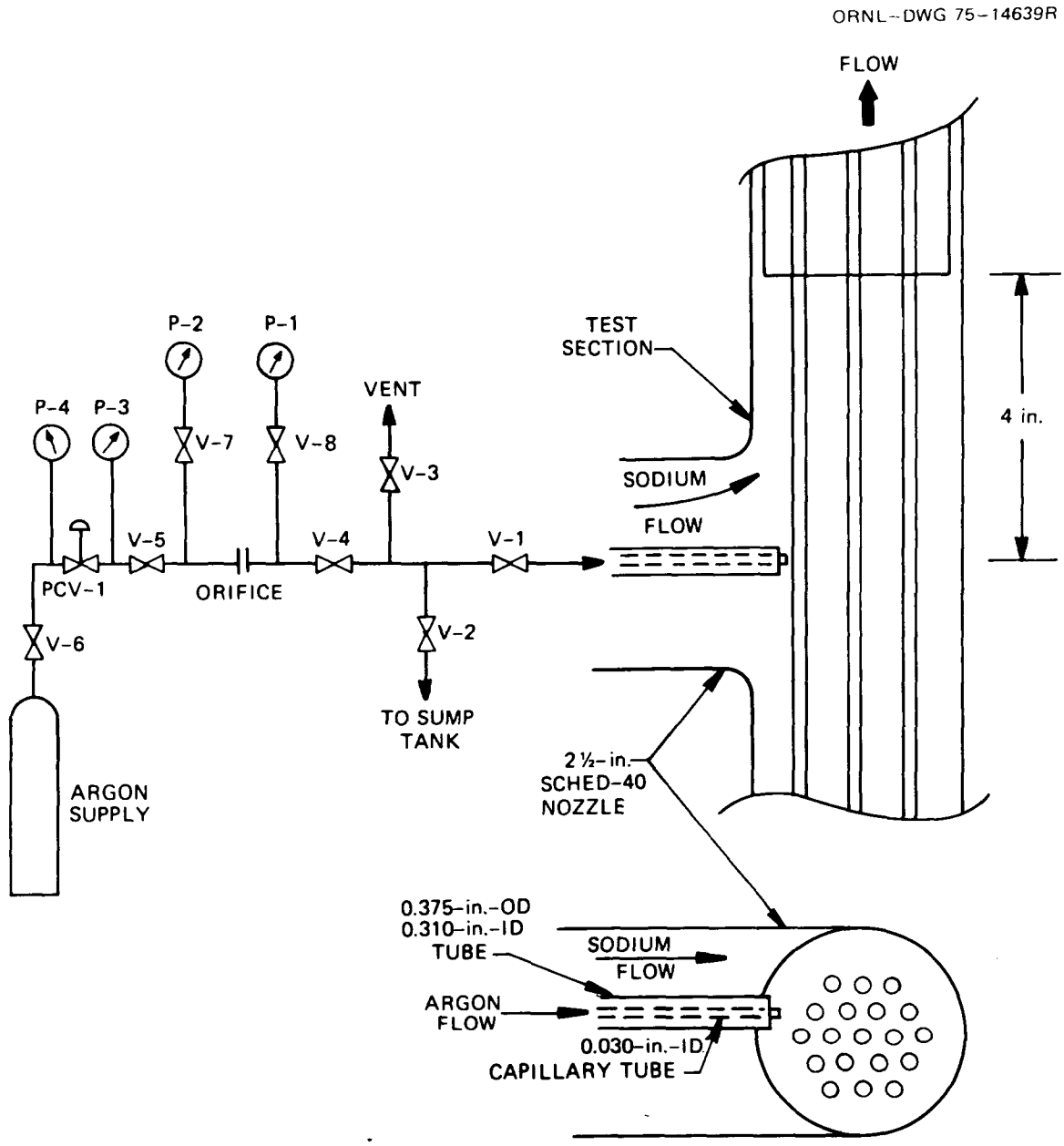

Fig. 5. Argon gas injection system for bundle 3B (1 in. = 25.4 mm).

Bundle 3B Instrumentation

The thermocouple instrumentation layout for bundle 3B is shown in Fig. 10. All thermocouples are fabricated from premium-grade Chromel-Alumel and are accurate to within ±0.5% of the actual temperature reading. With the use of pretest isothermal calibration techniques, temperatures may be measured to within ±3°C. The large circles represent the electrically heated

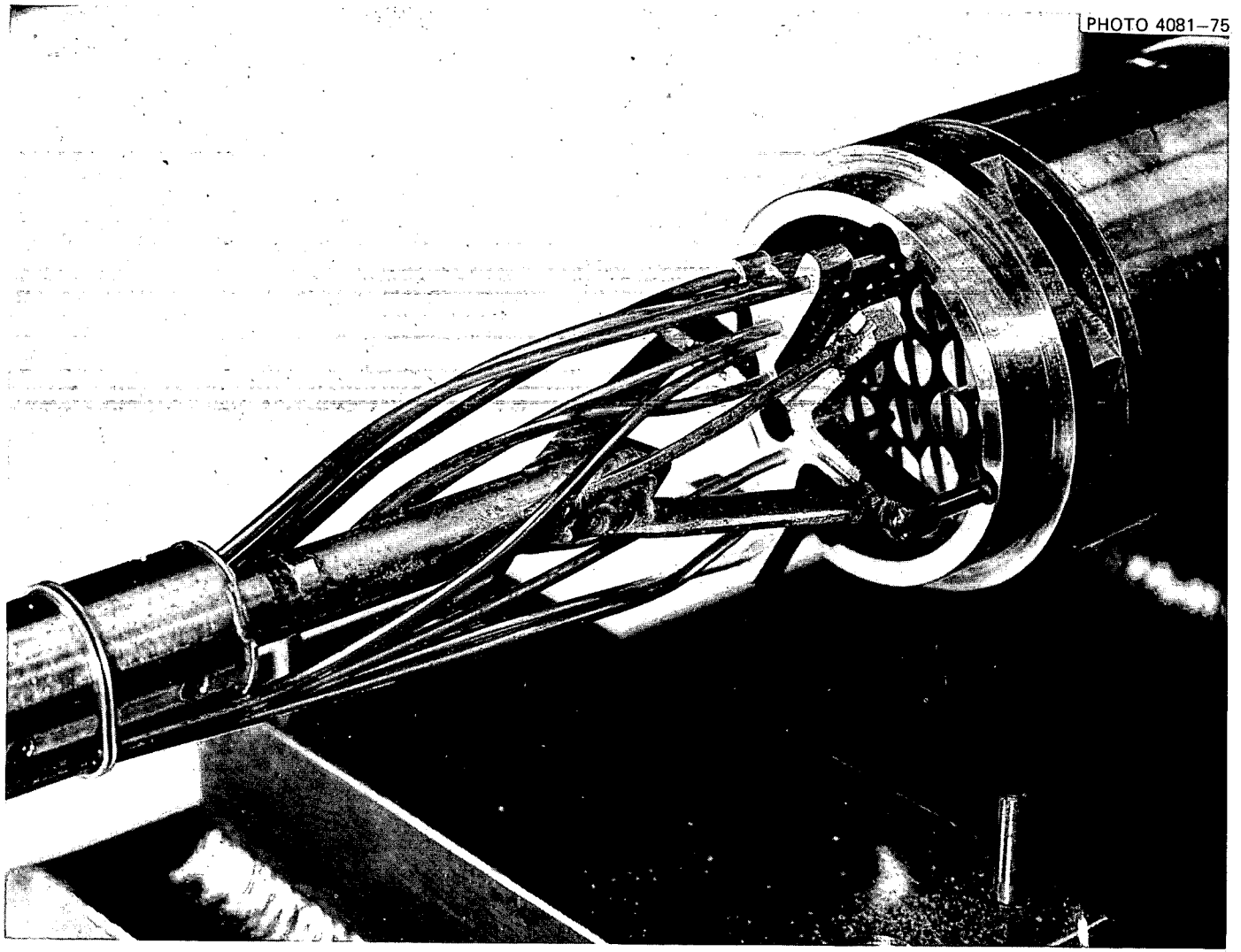

Fig. 6. Bundle 3B rake assembly and end of bundle just prior to installation in the facility.

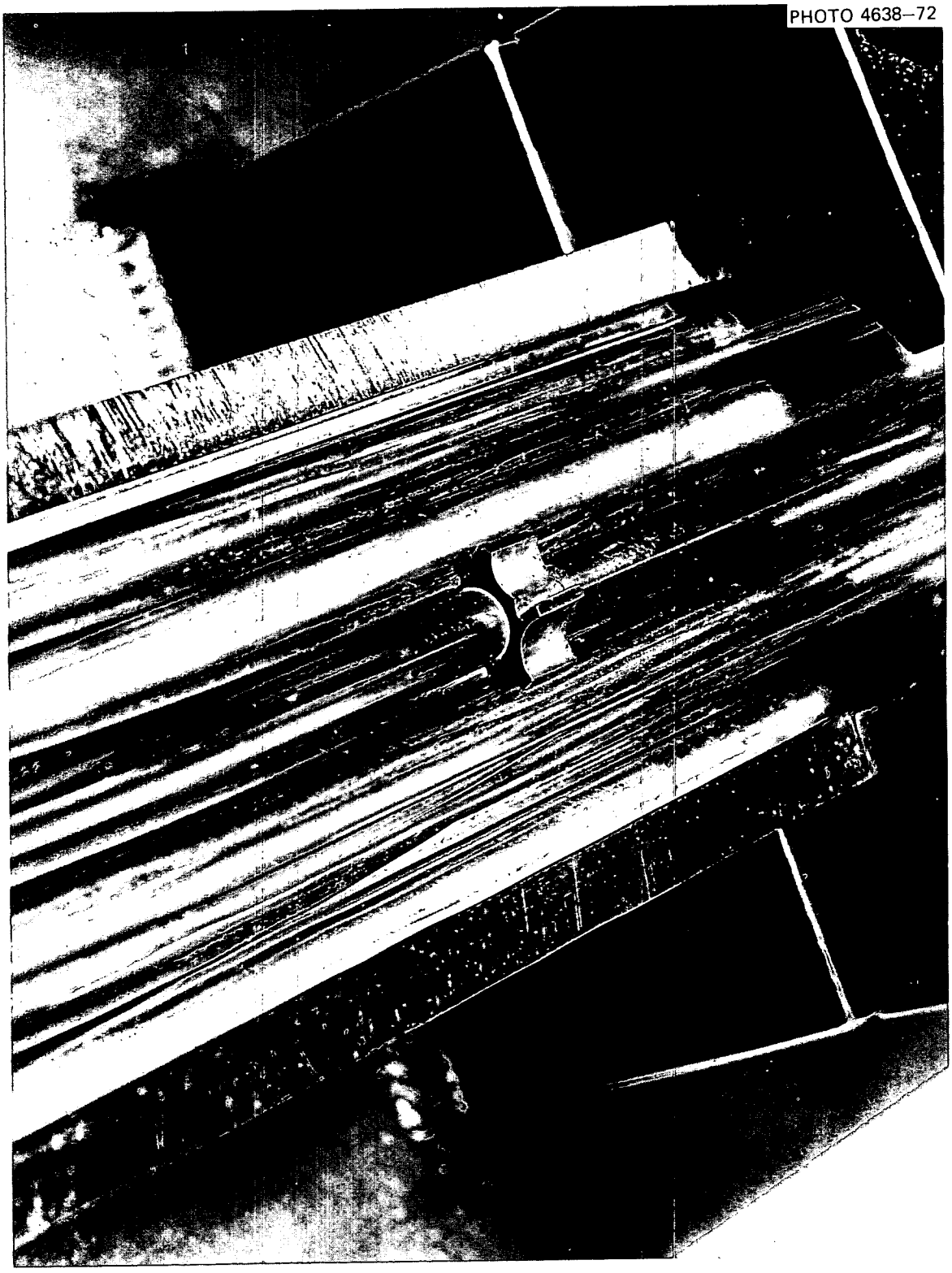

Fig. 7. Partially assembled bundle 3B, showing installation of fuel pin simulators adjacent to the blockage plate.

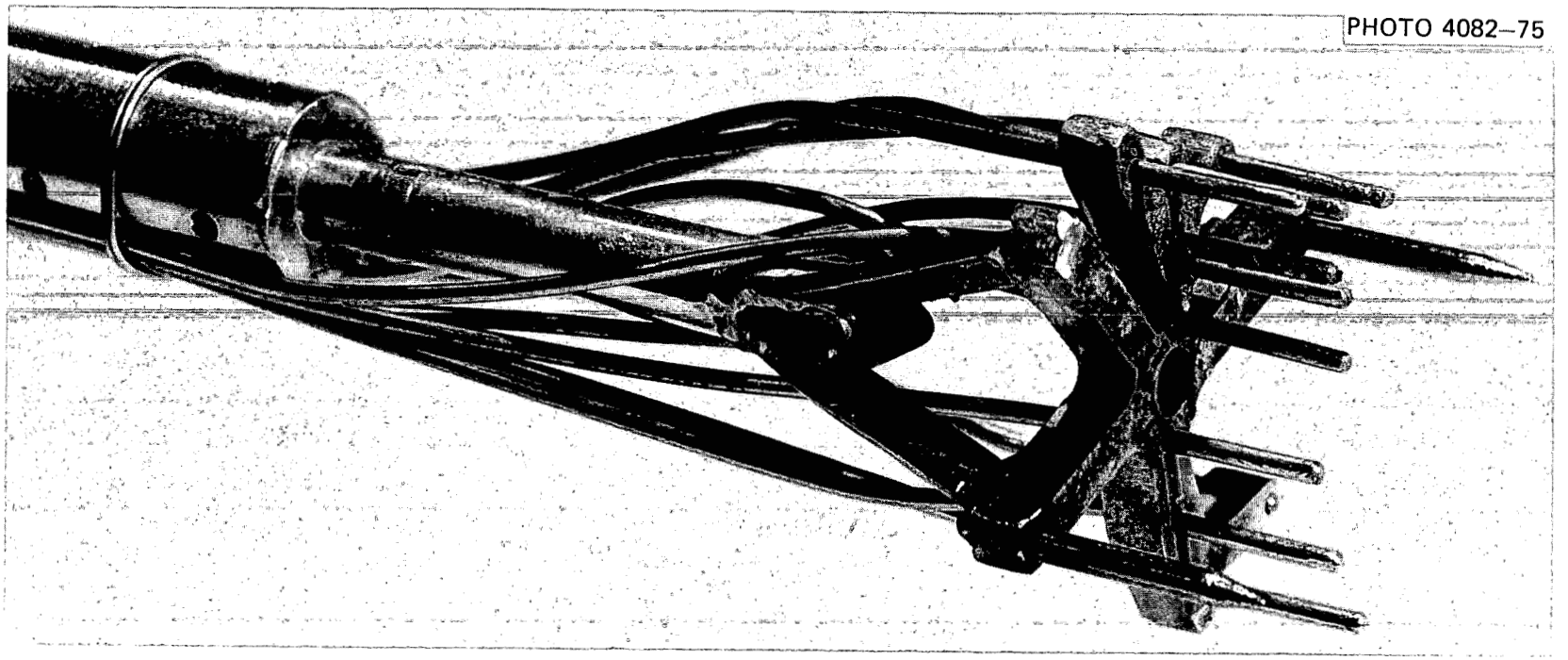

Fig. 8. Bundle 3B attemperator-rake assembly prior to installation in the facility.

PHOTO 4212–75

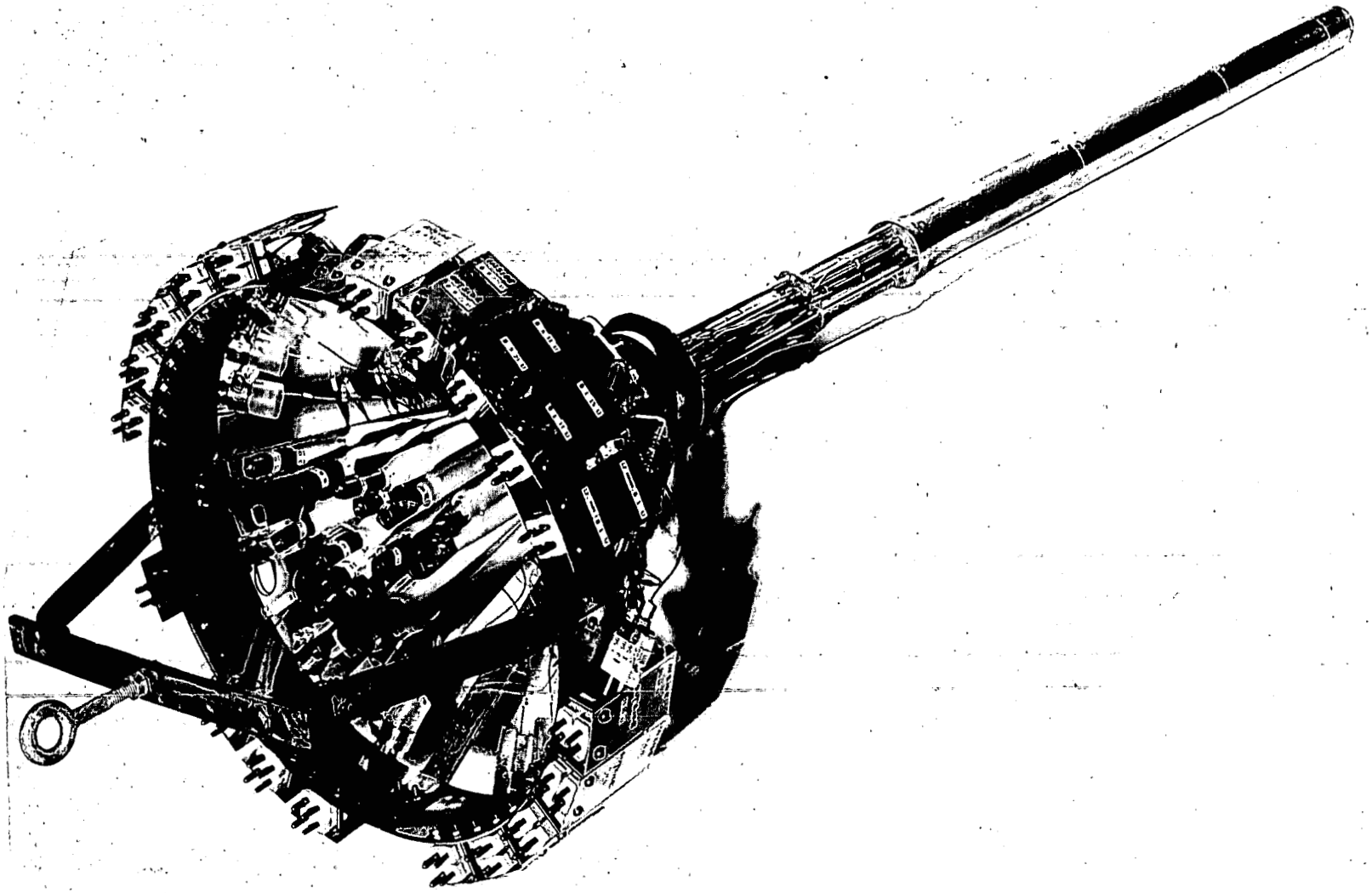

Fig. 9. Bundle 3B after removal from facility after test series 8 boiling tests.

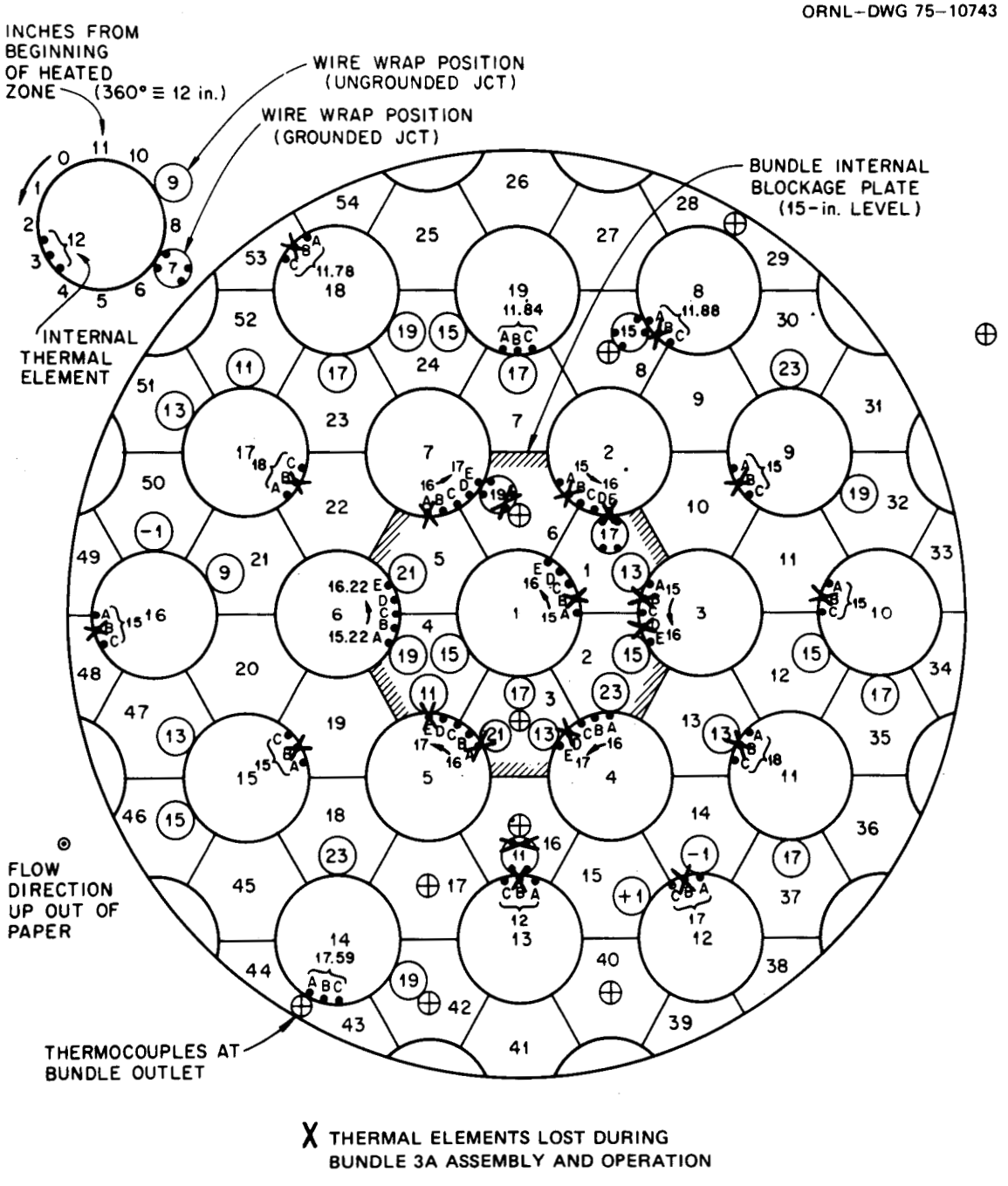

Fig. 10. Spacer wire and internal thermocouple locations for bundle 3B (1 in. = 25.4 mm).

fuel pin simulators; they are identified by the central number. The small tangent circles indicate the azimuthal position of the thermocouple junctions in the wire-wrap spacers. The thermocouple wires are insulated by compacted MgO swaged in an austenitic stainless steel sheath to the 1.42-mm-OD (0.056-in.) final wire-wrap dimension. The wire spacers wrapped

around each heater rod contain four thermal element wires; the wires are formed into either grounded or ungrounded temperature-measuring junctions that can be located at two axial locations. The thermocouple junctions are located at the axial levels indicated by the numbers in the small circles, which designate the number of inches from the start of the heated zone. The grounded junctions are designated by small circles containing pairs of dots (see wire wrap on heater 8). The pair of dots next to the heater surface indicates that a thermocouple junction in the wire wrap is adjacent to the heater, whereas the pair of dots on the opposite side indicates that the other junction, at the same axial level, measures temperatures near the center of the flow channel. The ungrounded-junction thermocouples are centrally located within the wire-wrap sheath and are at two axial locations (see a typical pair of grounded junctions in wire wrap on heater 1).

The flow channels, defined by the lines connecting the centers of the fuel pin simulators, are identified by the numbers in the segments so defined. The small circles with interior crosses indicate thermocouples located at the bundle exit.

The fuel pin simulators have thermal elements attached to the inner surface of the sheath as indicated by the dots labeled A, B, C, D, E. The ends of these thermal elements are located at 15° azimuthal intervals and at 6.55-mm (0.25-in.) axial intervals; thus the junction formed by two thermal elements in heaters 1, 2, and 3 measure temperatures from 381 to 406 mm (15 to 16 in.) from the start of the heated zone in 6.4-mm (0.25-in.) increments; those in heater 6 measure from 387 to 412 mm (15.22 to 16.22 in.); and those in heaters 4, 5, and 7 measure from 406 to 432 mm (16 to 17 in.).

All thermocouple junctions that gave unreliable responses prior to operation of bundle 3B are crossed out in Fig. 10 and were not used to record experimental data.

Bundle 3B Data Processing

Data were recorded with a fast data-acquisition system capable of recording 128 channels at 10,000 channels/sec. In the 22 tests with bundle 3B, the system scanned 84 channels at least every 0.1 sec and recorded the signals on magnetic tape for either 0.7 sec or 0.8 sec out of every 1.25

sec. The remaining 0.55 or 0.45 sec, during which no data were recorded, was used to display selected signals on an oscilloscope for visual monitoring. FORTRAN data-processing programs were used to process the data of all 79 instruments; the plots for all runs are presented in the bundle 3B data record.[13]

QUASI-STEADY-STATE BOILING DOWNSTREAM OF BLOCKAGE WITHOUT INERT-GAS INJECTION

Tests Conducted

Seven test runs, as shown in Table 1, were conducted in an effort to determine the effects of local boiling downstream of the blockage. Six of the tests (test 3, runs 101a–101f) consisted of decreasing the test-section flow at constant heater power just enough to initiate sodium boiling; thereafter the flow was kept constant. The saturation temperature for these tests was approximately 955°C (1750°F). The resulting quasi-steady-state boiling was maintained long enough to give consistent data without endangering the integrity of the fuel pin simulators. In test 4, heater power was varied in an attempt to suppress and initiate periods of quasi-steady-state boiling. Figures 11 and 12 show typical temperature, flow, and heater power responses during test 3 (run 101c) and test 4. These two tests were also chosen for analysis, since they contained the longest, most intense (lowest flow-to-power ratio) quasi-steady-state boiling periods (13 and 27 sec, respectively). Boiling conditions were most easily recognized from thermocouple responses during these two tests. The onset of boiling during the operation of the tests was determined by (1) monitoring all bundle thermocouple temperatures on a continuous cathode-ray tube (CRT) visual display [boiling was evident when the temperature exceeded the expected sodium saturation temperature of 955°C (1750°F)]; (2) monitoring the amplified audio signal from an electromagnetic microphone attached to the test-section housing for the already familiar (from bundle 5D boiling tests) "crackling" noise of sodium vapor bubble collapse, and (3) monitoring the response from sophisticated acoustic detection instruments (hydrophones and lithium niobate crystals).

Table 1. Quasi-steady-state boiling experiments without gas injection — test series 8 (bundle 3B)[a]

Initial test section flow = 1.4 liters/sec (22 gpm)
Initial heater power = 16.4 kW/m (5.0 kW/ft)

Test	Run No.	Date	Heaters operative	Test section inlet temperature [°C (°F)]	Uniform heater power[b] during quasi-steady-state boiling periods (kW/ft)	Avg. flow[c] during quasi-steady-state boiling periods (gpm)	Duration of quasi-steady-state boiling periods (sec)
3	101a	4-8-75	19	482 (900)	5.0	9.0	2
3	101b	4-8-75	19	493 (920)	5.0	9.0,8.0,8.5	2,3,2
3	101c	4-9-75	19	560 (1040)	5.0	9.6,9.0,8.2[d]	8,6,13[d]
3	101d	4-9-75	19	571 (1060)	5.0	8.9	16
3	101e	4-9-75	19	582 (1080)	5.0	8.9	4
3	101f	4-9-75	18[e]	560 (1040)	5.0	6.4,6.1	6,12
4 (modified)		4-10-75	18[e]	487 (910)	4.0,4.0,4.5,[d]5.0	6.0,5.6,5.6,[d]6.5	50,80,27,[d]20

[a]Conversion factors: 1 gpm = 0.063 liter/sec; 1 kW/ft = 3.28 kW/m.

[b]Peak Fast Flux Test Facility (FFTF) heater power = 14.1 kW/ft.

[c]100% FFTF flow (corresponding to a velocity of 24 fps) = 54 gpm in bundle 3B.

[d]Period selected for detailed analysis.

[e]Electric circuit of heater 7 was open during test.

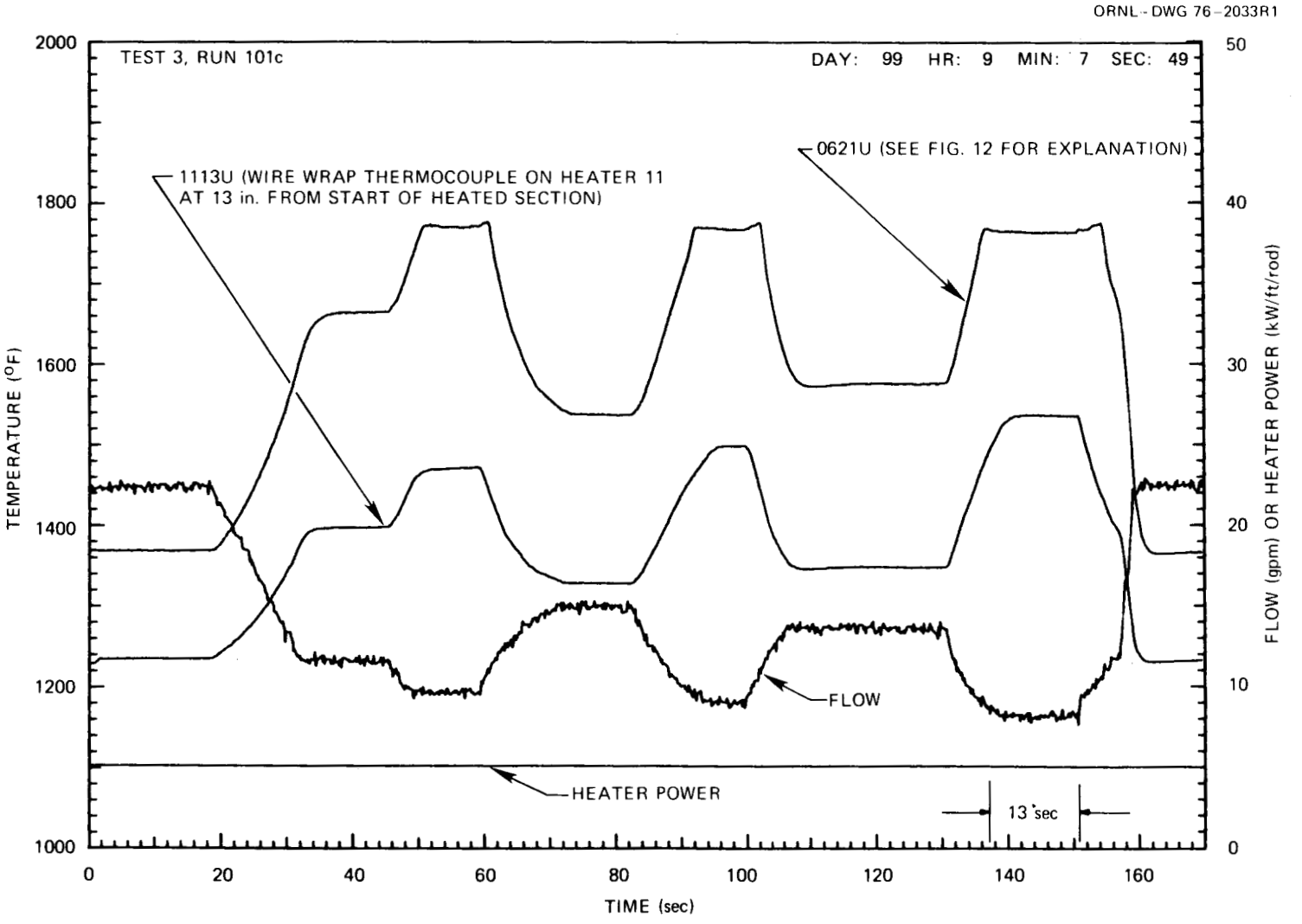

Fig. 11. Responses of electromagnetic flowmeter, average heater power, and two thermocouples for test 3, run 101c (1 gpm = 0.063 liter/sec; 1 kW/ft/rod = 3.3 kW/m/rod).

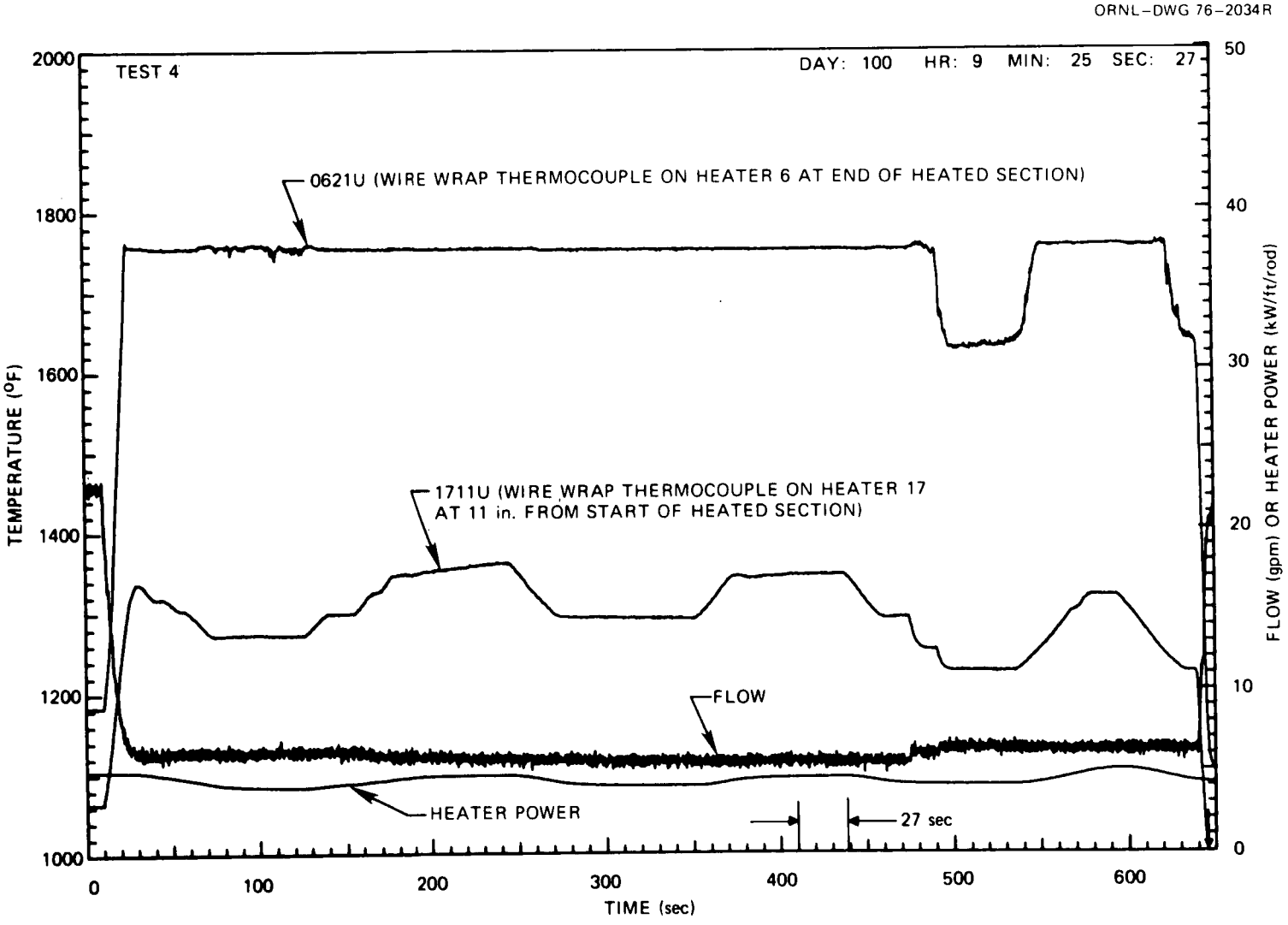

Fig. 12. Responses of flowmeter, average heater power, and two thermocouples for test 4 (1 gpm = 0.063 liter/sec; 1 kW/ft/rod = 3.3 kW/m/rod).

Determination of Vapor Bubble Generation from Thermocouple Responses

In order to establish the extent of vapor generation (or the subcooled boundaries of the vapor), several criteria were used to determine if a thermocouple response indicated the presence of sodium vapor near the thermocouple during the quasi-steady-state boiling periods.

If the temperature of a thermocouple is independent of a change in flow and/or power, it is assumed that the forced convection nucleate boiling regime has been entered. In Fig. 11, note the difference in the responses of wire-wrap thermocouples 0621U and 1113U during the three successively lower flow periods (50–60, 94–100, and 138–151 sec). Whereas the temperature plateaus of 1113U [51 mm (2 in.) upstream of the blockage] increase for each lower-flow period (indicating forced convection single-phase flow), the temperature plateaus of 0621U [152 mm (6 in.) downstream of the blockage] remain essentially constant during the three low-flow periods (indicating sodium vapor bubbles present at the wire-wrap surface). In Fig. 12, on the other hand, the heater power is varied while the flow remains essentially constant at approximately 0.38 liter/sec (6 gpm). Note the difference between the responses of two wire-wrap thermocouples (0621U and 1711U). The temperature of 1711U [at 102 mm (4 in.) upstream of the blockage] varies with heater power (indicating single-phase forced convection flow), while the temperature of 0621U remains essentially constant and independent of power variations from 25 to 490 sec (indicative of the forced convection nucleate boiling regime).

If the temperature of a thermocouple stabilizes prior to the time that the decreasing flow has reached its minimum, the temperature is also considered independent of flow and is an indication of boiling. An example of this is thermocouple 0621U in Fig. 9; its temperature reading stabilized at approximately 136 sec, which is 2 sec prior to the time at which the flow reached its lowest value.

If the temperature of a thermocouple reaches its highest plateau after the flow has reached its minimum value, the thermocouple temperature is compared to a calculated single-phase sodium saturation temperature. If the thermocouple temperature is well below this calculated saturation temperature (e.g., 1113U during the analyzed quasi-steady-state boiling period

shown in Fig. 11), it is designated as a "nonboiling" thermocouple. If the thermocouple temperature is approximately equal to or above the saturation temperature, its time of temperature stabilization is compared to that of "nonboiling" thermocouples. Thus, for thermocouples that reach their temperature plateaus near the saturation temperature prior to the time that a "nonboiling" thermocouple does, the presence of sodium vapor in their vicinity is considered established. If they reach their temperature plateaus near the saturation temperature after a typical "nonboiling" thermocouple, no definite conclusion as to the presence of vapor in the vicinity can be made.

Presentation of Test Results

The test results of the two quasi-steady-state boiling periods investigated are presented in Table 2 and in Figs. 13 and 14. All reliable responses from the thermocouples located between 330 mm (13.0 in.) and 584 mm (23.0 in.) from the start of the heated section were analyzed (Table 2). Temperatures of the nearest surface in contact with sodium at a particular thermocouple location were calculated as follows in the table: for internal heater thermocouples (R prefix), it was assumed that the heat flux in the heater cladding travels radially outward in a uniform manner around the heater circumference. For thermocouples in the center of wire wraps (those with U suffix), it was assumed that the temperature drop from the center of the wire wrap to the wire surface was half the measured temperature drop across one entire wire wrap at the 431-mm (17.0-in.) location (see measured temperatures of thermocouples 0217A and 0217B in Table 2). Wire-wrap thermocouple temperatures at the unheated 584-mm (23.0-in.) level, as well as those on the failed heater 7 (thermocouple 0719A in Table 2), were assumed to be the same as those on the wire-wrap surface, since there is very little radial heat conduction in the unheated portion of the rods at the end of the quasi-steady-state period analyzed. Temperatures from exit rake thermocouples [at 615 mm (24.2 in.) downstream from the start of the heated section] are not included in Table 2 because the large temperature fluctuations (±6 to ±70°C) during the quasi-steady-state period could not be easily analyzed; however, they are included in Figs. 13 and 14.

Table 2. Results of bundle 3B quasi-steady-state boiling tests (without gas injection)

Distance from start of heated section [mm (in.)]	Thermocouple[a]	Test 3, run 101c: Measured temperature at end of period [°C (°F)]	Test 3, run 101c: Estimated surface temperature at end of period [°C (°F)]	Test 3, run 101c: Evidence of vapor generation during period	Test 3, run 101c: Time of temperature stabilization[b] for period (sec)	Test 4: Measured temperature at end of period [°C (°F)]	Test 4: Estimated surface temperature at end of period [°C (°F)]	Test 4: Evidence of vapor generation during period	Test 4: Time of temperature stabilization[b] for period (sec)
		Flow: 0.52 liter/sec (8.2 gpm) (15% nominal flow) Heater power: 16.4 kW/m (5.0 kW/ft) Inlet temperature: 560°C (1040°F) Time of quasi-steady-state boiling period: 137.6–150.5 sec				Flow: 0.35 liter/sec (5.6 gpm) (10% nominal flow) Heater power: 14.8 kW/m (4.5 kW/ft) Inlet temperature: 488°C (910°F) Time of quasi-steady-state boiling period: 410.2–436.8 sec			
Blocked region									
381 (15.0)	0115U	924 (1695)	927 (1700)	No	141.6	960 (1760)	960 (1760)	?	406.3
381 (15.0)	0315U	910 (1670)	913 (1675)	No	141.9	954 (1750)	954 (1750)	?	383.9
390 (15.35)	R0115AD	968 (1775)	954 (1750)	?	141.5	unreliable			
390 (15.35)	R0615AB	979 (1795)	966 (1770)	?	142.6	977 (1790)	963 (1765)	Yes	370.3
391 (15.38)	R0215AD	935 (1715)	921 (1690)	?	141.3	957 (1755)	943 (1730)	?	407.8
396 (15.60)	R0615BC	966 (1770)	952 (1745)	Yes	140.7	960 (1760)	946 (1735)	Yes	365.4
397 (15.63)	R0215CB	977 (1790)	963 (1765)	Yes	138.2	unreliable			
397 (15.63)	R0116CD	977 (1790)	963 (1765)	Yes	136.4	977 (1790)	963 (1765)	Yes	366.3
303 (15.85)	R0616CD	974 (1785)	960 (1760)	Yes	139.0	968 (1775)	954 (1750)	Yes	372.8
403 (15.88)	R0116DE	977 (790)	963 (1765)	Yes	138.1	unreliable			
409 (16.10)	R0616DE	974 (1785)	960 (1760)	Yes	139.5	971 (1780)	957 (1755)	Yes	370.4
410 (16.13)	R0416AB	971 (1780)	957 (1755)	Yes	140.1	968 (1775)	954 (1750)	Yes	370.0
416 (16.38)	R0716BC	982 (1800)	968 (1775)	Yes	140.1	unreliable			
416 (16.38)	R0416BC	971 (1780)	957 (1755)	Yes	138.8	966 (1770)	952 (1745)	Yes	367.5
416 (16.38)	R0516BC	996 (1825)	982 (1800)	Yes	140.2	988 (1810)	974 (1785)	Yes	363.7
422 (16.63)	R0417BE	974 (1785)	960 (1760)	Yes	138.3	968 (1775)	954 (1750)	Yes	351.2
422 (16.63)	R0517CD	996 (1825)	982 (1800)	Yes	140.1	988 (1810)	974 (1785)	Yes	362.8
422 (16.63)	R0717BE	991 (1815)	977 (1790)	Yes	139.0	unreliable			
432 (17.0)	0117U	963 (1765)	960 (1760)	Yes	138.8	957 (1755)	954 (1750)	Yes	351.4
432 (17.0)	0217A	966 (1770)	963 (1765)	Yes	139.3	960 (1760)	957 (1755)	Yes	364.2
432 (17.0)	0217B	963 (1765)	963 (1765)	Yes	138.3	957 (1755)	947 (1755)	Yes	351.2
483 (19.0)	0619U	966 (1770)	963 (1765)	Yes	138.3	957 (1755)	954 (1750)	Yes	356.2
483 (19.0)	0719A	966 (1770)	963 (1765)	Yes	137.6	954 (1750)	954 (1750)	Yes	361.2
533 (21.0)	0521U	963 (1765)	960 (1760)	Yes	138.2	957 (1755)	954 (1750)	Yes	∿143
533 (21.0)	0621U	966 (1760)	957 (1755)	Yes	136.3	951 (1750)	952 (1745)	Yes	∿24
584 (23.0)	0423U	929 (1705)	929 (1705)	Yes	136.3	952 (1745)	952 (1745)	Yes	371.2
Unblocked region									
330 (13.0)	0313U	857 (1575)	854 (1570)	No	140.5	899 (1650)	896 (1645)	No	432.5
330 (13.0)	0413U	854 (1570)	852 (1565)	No	140.4	904 (1660)	902 (1655)	No	409.3
330 (13.0)	1113U	835 (1535)	832 (1530)	No	140.7	868 (1595)	866 (1590)	No	426.3
330 (13.0)	1513U	793 (1460)	791 (1455)	No	141.3	824 (1515)	821 (1510)	No	422.8
330 (13.0)	1713U	749 (1380)	746 (1375)	No	143.9	732 (1350)	729 (1345)	No	427.6
381 (15.0)	0815A	857 (1575)	860 (1580)	No	142.6	885 (1625)	885 (1625)	No	406.2
381 (15.0)	0815B	860 (1580)	860 (1580)	No	141.7	885 (1625)	885 (1625)	No	410.6
381 (15.0)	1015U	860 (1580)	863 (1585)	No	142.6	899 (1650)	898 (1650)	No	407.8
381 (15.0)	1515U	774 (1425)	777 (1430)	No	145.3	793 (1460)	793 (1460)	No	409.0
381 (15.0)	1915U	871 (1600)	874 (1605)	No	142.7	846 (1555)	846 (1555)	No	424.4
432 (17.0)	1017U	849 (1560)	846 (1555)	No	142.8	938 (1720)	935 (1715)	No	400.2
432 (17.0)	11117U	824 (1515)	821 (1510)	No	147.6	879 (1615)	877 (1610)	No	406.9
432 (17.0)	1817U	893 (1640)	891 (1635)	No	145.1	863 (1585)	860 (1580)	No	408.8
432 (17.0)	1917U	932 (1710)	929 (1705)	?	142.6	929 (1705)	927 (1700)	No	409.2
447 (17.59)	R1418AB	821 (1510)	807 (1485)	No	145.4	unreliable			
447 (17.59)	R1418BC	829 (1525)	816 (1500)	No	145.6	unreliable			
483 (19.0)	0919U	868 (1595)	866 (1590)	No	145.1	938 (1720)	935 (1715)	No	401.9
483 (19.0)	1419U	896 (1645)	893 (1640)	No	143.9	907 (1665)	904 (1660)	No	408.8
483 (19.0)	1819U	960 (1760)	957 (1755)	?	141.8	949 (1740)	946 (1735)	?	399.2
584 (23.0)	0923U	910 (1670)	910 (1670)	No	145.4	949 (1740)	949 (1740)	Yes	369.3
584 (23.0)	1423U	854 (1570)	854 (1570)	No	145.5	949 (1740)	949 (1740)	Yes	382.8

[a] Numbers of wire-wrap thermocouples consist of four digits followed by a single letter (e.g., 0315U, 0217A, and 0217B). The first two digits give the heater number (see Fig. 10) adjacent to the wire wrap, the second two digits give the axial location downstream of the start of the heated section, and the single letter stands for the physical location inside the wire wrap (i.e., U indicates an ungrounded type in the center of the wire wrap, A indicates a grounded thermocouple adjacent to the heater, and B indicates a grounded type adjacent to sodium). Numbers of grounded heater internal thermocouples start with the letter R and are followed by four digits for the heater number and the axial location downstream from the start of the heated section; the final two letters indicate the thermal elements which form the thermocouple junction.

[b] Temperature stabilization is defined as being reached whenever 99% of total temperature rise is reached during flow coastdown or power increase.

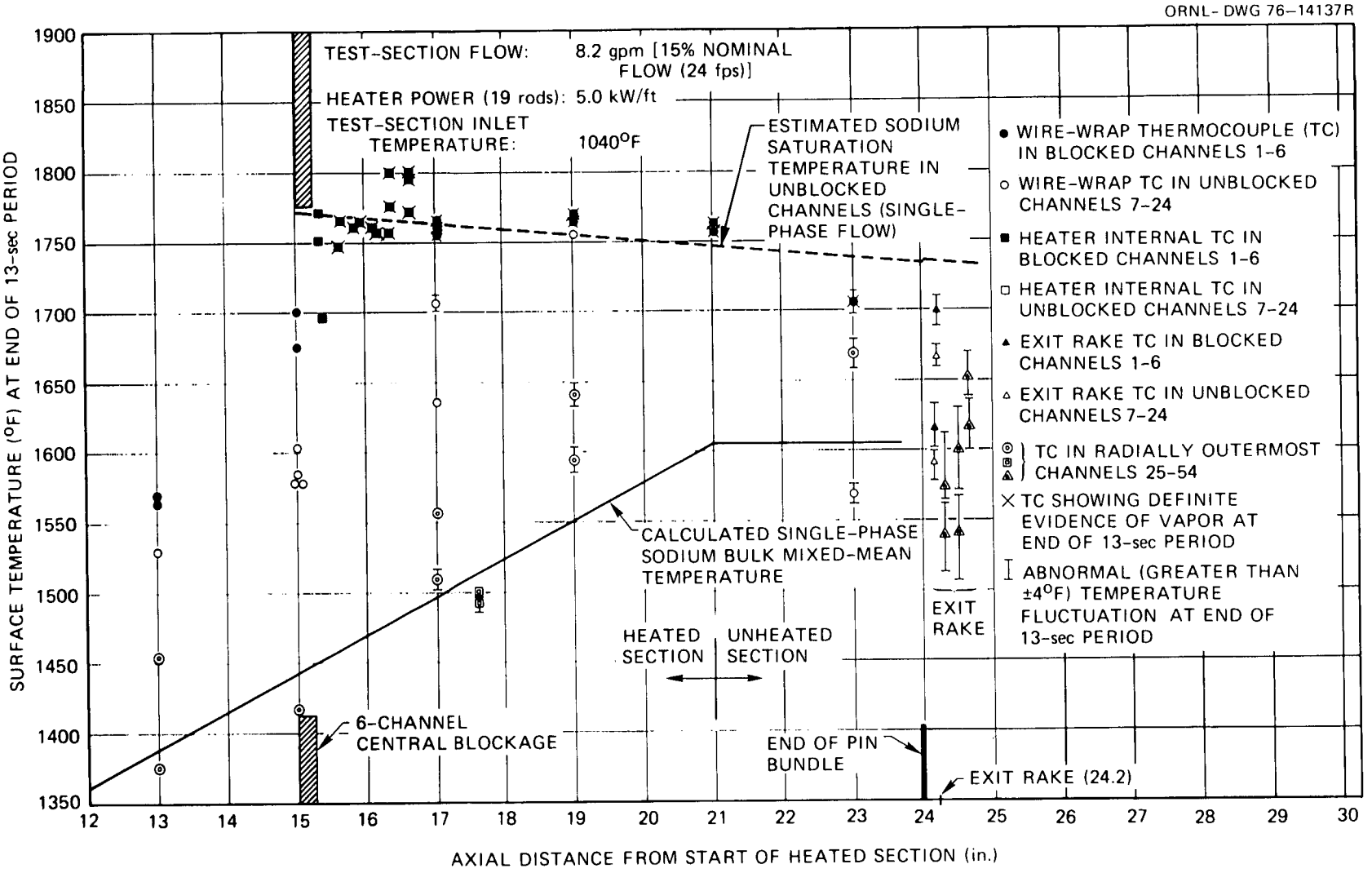

Fig. 13. Experimental temperatures in vicinity of blockage at end of 13-sec period in test 3, run 101c (1 gpm = 0.063 liter/sec; 1 kW/ft = 3.28 kW/m; 1 fps = 0.3048 m/sec; 1 in. = 25.4 mm).

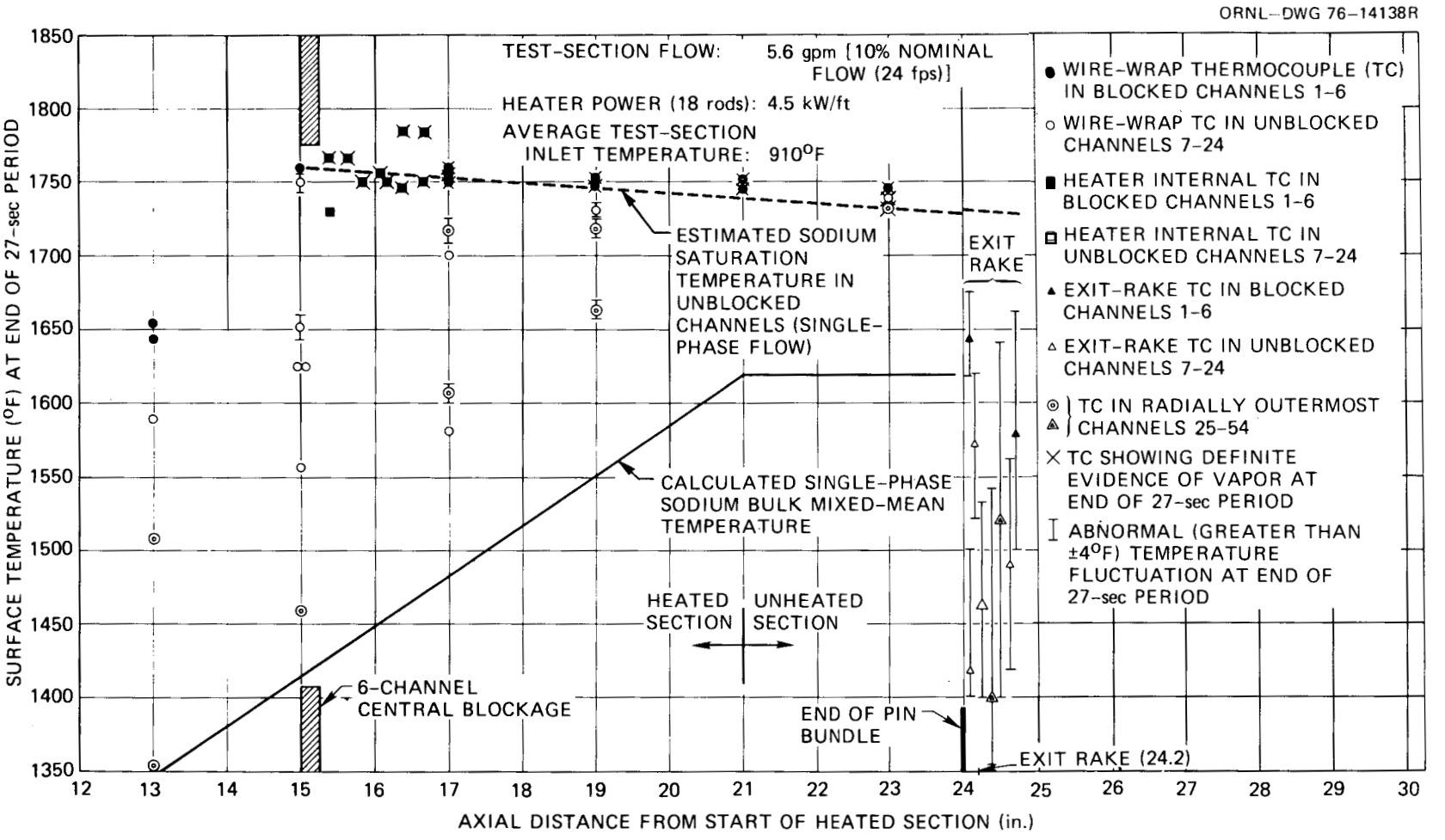

Fig. 14. Experimental temperatures in vicinity of blockage at end of 27-sec period in test 4 (1 gpm = 0.063 liter/sec; 1 kW/ft = 3.28 kW/m; 1 fps = 0.3048 m/sec; 1 in. = 25.4 mm).

Figures 13 and 14 include a single-phase sodium saturation temperature that was calculated for the quasi-steady-state condition with a simple computer program. Basically, the program calculates the single-phase axial test-section pressure profile, given the experimental pressures at the inlet and outlet of the test section. However, in the suspected two-phase region between the blockage and the attemperator, a linear axial pressure profile is assumed, since the sodium void fraction and flow behavior in this region could not be established from bundle 3B results.

The sodium bulk temperature shown in Figs. 13 and 14 is calculated from a simple heat balance by assuming no blockage and no two-phase flow.

Discussion of Test Results

Axial propagation of the local boiling zone

In regard to the radial or axial propagation of the local boiling zone during quasi-steady-state boiling, it must be pointed out that axial propagation in a reactor subassembly could not be investigated with the results of bundle 3B tests because of the existence of several nonprototypicalities in the THORS test facility. In particular, upstream propagation of the void during quasi-steady-state boiling periods was not likely in the THORS facility because the test-section flow was not significantly reduced by an increase in test-section pressure drop as in LMFBR subassemblies. The flow in the THORS tests was throttled at the test-section inlet, and the major portion of the loop pressure loss occurred at that point. Downstream propagation of the local boiling zone was limited by an attemperator, which injected "cold" sodium (at test-section inlet temperature) into the two-phase sodium flow at approximately 305 mm (12 in.) downstream of the blockage (see Fig. 4). Consequently, the attemperator flow condensed essentially all sodium vapor. A large portion of the temperature fluctuation at the farthest measuring point downstream of the blockage (see exit rake thermocouples in Figs. 5 and 6) is a result of the flow agitation caused by vapor collapse. Some temperature fluctuations have been observed that can be attributed to the movement of heater rods, which actually changed the configuration of the flow channel.

The initiation sequence of vapor generation prior to the quasi-steady-state periods as a function of time and axial position can be determined from the temperature stabilization column in Table 2 and is given in Table 3. The results show that vapor generation is first initiated at the end of the heated section [533 mm (21 in.)] and is later detected throughout the blockage wake. For a constant axial power profile, the end of the heated section is expected to be the first area to experience the highest local sodium temperature (saturation temperature) during a flow or power transient. The sodium in the blockage wake region [first 51 mm (2 in.) downstream of the blockage] reaches saturation temperatures several seconds later than the sodium at the end of the heated zone because of the initially lower bulk temperatures in the wake. Flow recirculation in the wake zone heats the sodium there to the point of saturation (and boiling).

A spontaneous burst of sodium bubbles or of a single large bubble in the wake zone (indicative of a large sodium superheat) is not evident from the results shown in Tables 2 and 3. Temperatures measured in the blocked, heated channels from 381 to 533 mm (15 to 21 in.) show that vapor generation did not start throughout the blockage wake at the same time. Instead, as much as 4 sec elapse during test 3, run 101c, and as much as 21 sec elapse in test 4 before vapor envelopes the entire blockage wake.

Radial propagation of the local boiling zone

The results of test 3, run 101c (Table 2), show that during the 13-sec quasi-steady-state period, definite evidence of sodium vapor was found only in the blocked region of the bundle (channels 1 to 6 in Fig. 10). One wire-wrap thermocouple in the unblocked channels [1819U at the 483-mm (19-in.) level on heater 18] showed a temperature near the sodium saturation temperature, but none of the criteria for evidence of vapor generation was applicable. Even though this temperature is close to the saturation temperature, the major point is that all temperatures in the unblocked channels had stabilized at least 3 sec prior to the end of the boiling period. The stable temperatures reached in the unblocked channels after 10 sec of quasi-steady-state boiling and the large amount of subcooling in the outermost flow channels [$T_{sat} - T_{minimum\ measured}$), see Fig. 13] indicate that the local boiling zone did not propagate from the blocked to the unblocked channels during the 13-sec quasi-steady-state period analyzed.

Table 3. Initiation sequence of continuous vapor generation prior to quasi-steady-state boiling periods

Distance from start of heated section[a] [mm (in.)]	Thermocouple[b]	Time of temperature stabilization (seconds into run)
Test 3, run 101c		
533 (21)	0621U	136.3
584 (23)	0423U	136.3
397 (15.63)	RO116CD	136.4
Start of quasi-steady-state boiling period		137.6
483 (19)	0719U	137.6
403 (15.88)	RO116DE	138.1
533 (21)	0521U	138.2
397 (15.63)	RO215CD	138.2
422 (16.63)	RO417BE	138.3
Test 4		
533 (21)	0621U	24
533 (21)	0521U	143
432 (17)	0217B	351.2
422 (16.63)	RO417BE	351.2
432 (17)	0117U	351.4
483 (19)	0619U	356.2
483 (19)	0719A	361.2
422 (16.63)	RO717BE	362.8
Start of quasi-steady-state boiling period		410.2

[a]Blockage is located 381 mm (15.0 in.) from start of heated section.

[b]See footnote to Table 2 for an explanation of thermocouple numbering system.

The results of test 4 (Table 2) with 18 heaters powered (the heating element of pin 7 had failed during the earlier boiling tests) were essentially the same as those of test 3, run 101c, except for the two wire-wrap thermocouples at the unheated, unblocked 584-mm (23-in.) level. This difference is primarily due to the lower flow/power ratio in test 4, which results in the 20% less subcooling $[T_{sat} - T_{bulk})_{single\text{-}phase}]$ observed at this level in test 4 (see Figs. 13 and 14). Vapor that is swept out from the blocked channels to the unblocked channels at the 584-mm (23-in.) level does not encounter sodium at temperatures low enough to cause complete condensation. Therefore, radial propagation of the vapor zone in bundle 3B may have occurred to a limited extent in the unheated section of the bundle at 205 mm (8.0 in.) downstream of the blockage. However, in the first 103 mm (4.0 in.) downstream of the blockage (which includes the blockage wake), the results of test 4 do not indicate radial propagation of the local boiling zone. Local boiling zone stability at the end of the quasi-steady-state boiling period is found in the results from test 4 by examining the time of temperature stabilization listed in Table 2. All temperatures in the unblocked region (downstream of the blockage) had stabilized at least 13 sec prior to the end of the 27-sec quasi-steady-state boiling period.

Dryout in Local Boiling Zone

Surface temperatures at dryout locations would be expected to increase sharply [above 982°C (1800°F)] as the liquid film on the pin surface evaporates completely. None of the thermocouples that indicated the presence of vapor in their vicinity exhibited this behavior during the quasi-steady-state boiling periods investigated.

CONCLUSIONS CONCERNING BUNDLE 3B QUASI-STEADY-STATE BOILING

Axial propagation of the sodium vapor zone in the 6-channel blockage wake was limited in both axial directions by the test facility design.

Evidence of radial propagation of the sodium vapor zone from the blocked to the unblocked channels was not found during the 13-sec quasi-steady-state period investigated. Although two thermocouples in the unblocked channels [at 51 mm (2 in.) and 102 mm (4 in.) downstream of the

blockage] were close to the estimated sodium saturation temperature, evidence of sodium vapor could not be established. Stable temperatures were reached by all thermocouples in the unblocked channels 3 sec prior to the end of the 13-sec period.

No evidence of radial propagation of the local boiling zone in the first 103 mm (4.0 in.) downstream of the blockage was found during the 27-sec quasi-steady-state boiling period, although one thermocouple in an unblocked channel at 103 mm (4 in.) downstream of the blockage was close to the saturation temperature. Evidence of sodium vapor was found in the unblocked channels at the unheated 203-mm (8-in.) position downstream of the blockage, indicating that radial propagation of sodium vapor could have occurred there to a limited extent. Stable temperatures were reached by all thermocouples in the unblocked channels 13 sec prior to the end of the 27-sec period.

No evidence of sharp temperature increases leading to dryout was found on any heated pin surface during either the 13-sec or the 27-sec quasi-steady-state boiling periods investigated.

EXTRAPOLATION OF CONCLUSIONS TO LMFBR SUBASSEMBLIES

The conclusions reached for quasi-steady-state boiling in a 19-rod centrally blocked bundle are significant to LMFBR safety only to the extent that they can be extrapolated to full-scale 217-pin fuel subassemblies.

Bundle 3B test results could not give an insight into axial propagation of the boiling zone in the wake because of the nonprototypicalities in the THORS facility.

In order to apply the radial boiling propagation results from bundle 3B to a 217-pin LMFBR subassembly, a comparison of idealized radial temperature profiles at 25 mm (1.0 in.) downstream of the blockage is shown in Fig. 15 for both bundle 3B and a 217-pin bundle, where the bundle cross sections are subdivided into ringlike parallel flow channels. The temperature profile in the 217-pin assembly is hypothetically stipulated by assuming that a 6-channel blockage in a 217-pin bundle [100% nominal flow and 46 kW/m (14 kW/ft) heater power] has caused the sodium in the wake to approach its saturation temperature to the same degree as in the case of bundle 3B [10%

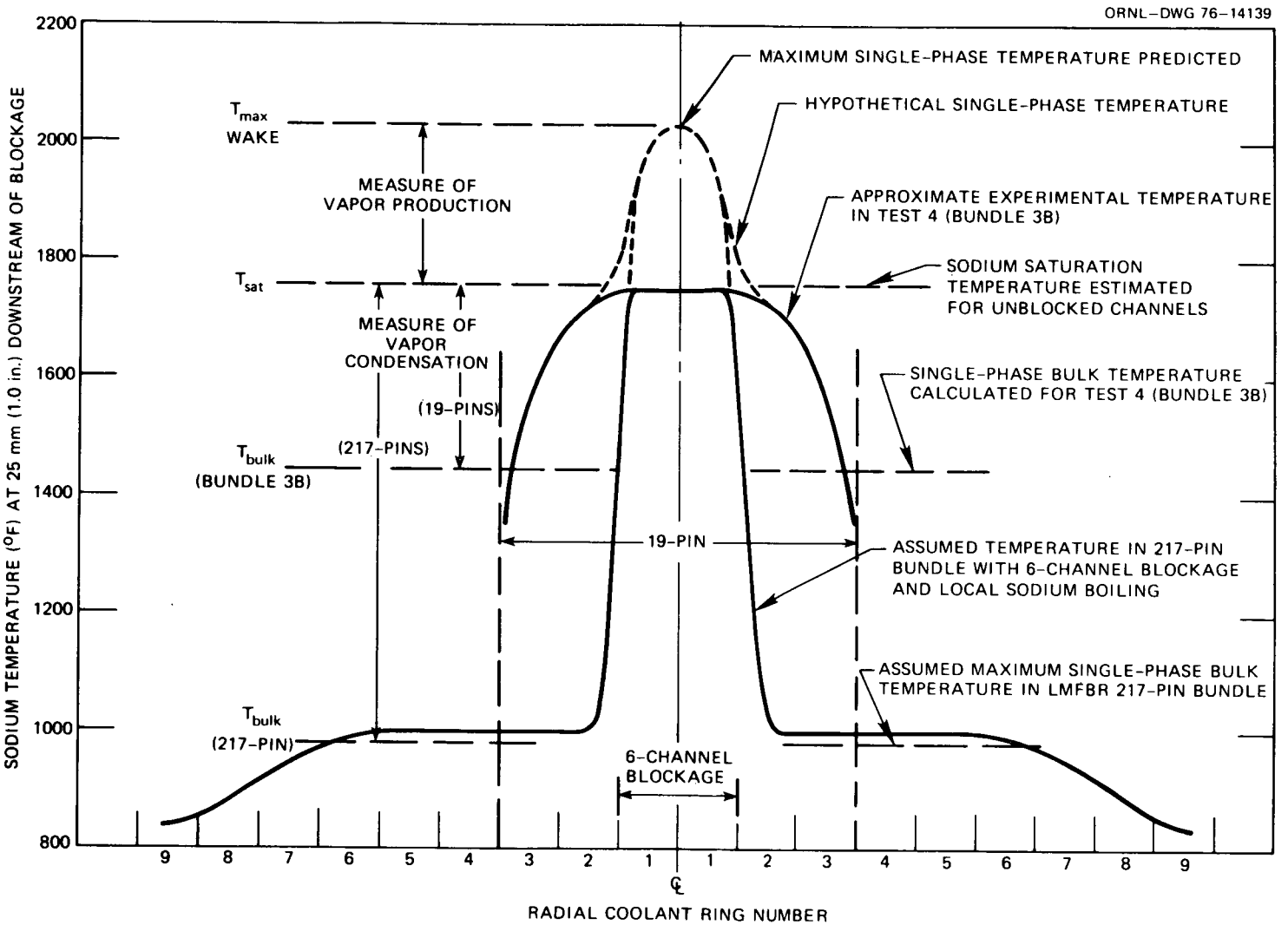

Fig. 15. Idealized radial temperature profiles during quasi-steady-state boiling with 6-channel blockage [°C = 5/9 (°F - 32)].

nominal flow and 15 kW/m (4.5 kW/ft) heater power]. The dotted temperature profiles in Fig. 15 define a hypothetical maximum single-phase sodium temperature in the wake, which was predicted as a function of flow and power from experimental single-phase THORS data as shown by Han et al.[14] in Fig. 16.

If a radial stability factor for radial boiling propagation is then defined as the ratio of the vapor-condensing capability (restraining force) to the vapor-producing capability (driving force), $[T_{sat} - T_{bulk})/(T_{max\ wake} - T_{sat})]_{single\ phase}$, a quantitative comparison can be made between bundle 3B results and a hypothetical 6-channel blockage temperature profile in a 217-pin bundle, as shown in Table 4. If one assumes that the saturation temperatures around the wake are the same in both the 19-pin and 217-pin bundles, the radial stability factor in the 217-pin bundle is calculated to be greater than that of test 3, run 101c, and test 4 by factors of

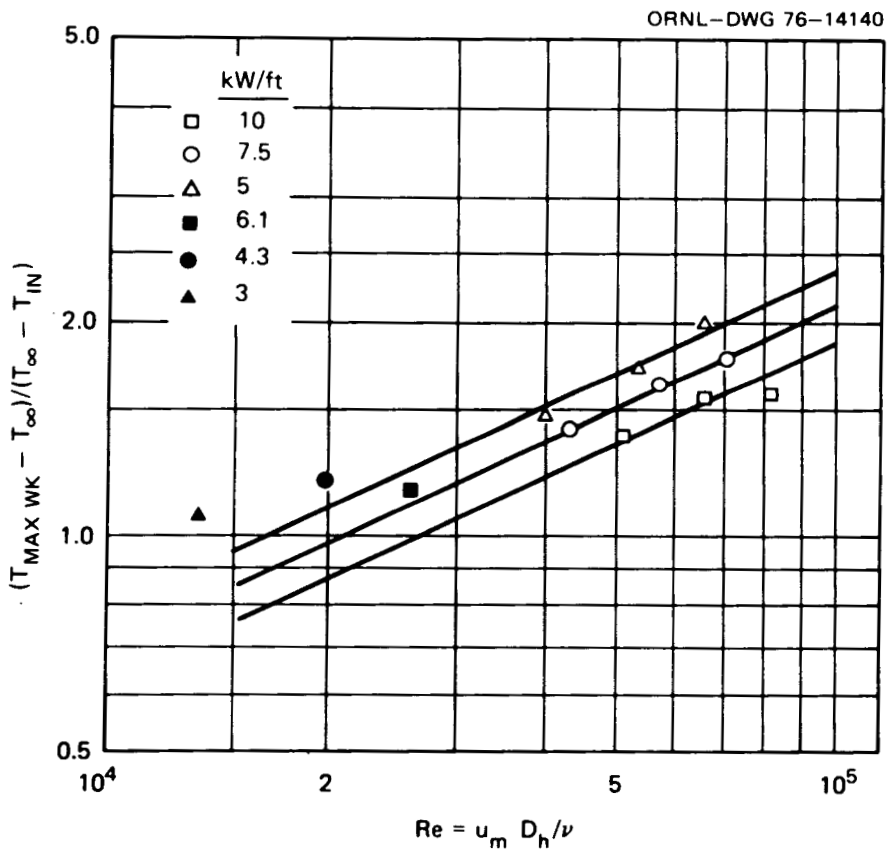

Fig. 16. Maximum temperature prediction in wake of 6-channel blockages (1 kW/ft = 3.28 kW/m).

Table 4. Radial boiling propagation for the wake of 6-channel blockages during quasi-steady-state boiling

Experiment	Bundle size	Nominal flow (%) / Uniform heater power[a] (kW/ft)	Inlet/outlet temperature [°C/°C (°F/°F)]	Calculated single-phase bulk temperature [°C (°F)]	Calculated sodium saturation temperature [°C (°F)]	Predicted single-phase maximum wake temperature[b] [°C (°F)]	Radial stability factor $\left(\frac{T_{sat} - T_{bulk}}{T_{max\ (wake)} - T_{sat}}\right)_{single\ phase}$
Test 3, run 101c	19	15 / 5.0	560/874 (1040/1605)	800 (1470)	965 (1765)	1060 (1940)	1.7
Test 4	19	10 / 4.5	488/882 (910/1620)	790 (1450)	960 (1755)	1110 (2030)	1.1
LMFBR (hypothetical 6-channel blockage with local sodium boiling)	217	100 / 14.0	316/527 (600/980)	525 (980) (assumed maximum)	960 (1755) (assumed same as test 4	1110 (2030) (assumed same as test 4	2.8

[a] Conversion factor: 1 kW/ft = 3.28 kW/m.

[b] See Ref. 14.

1.7 and 2.8, respectively. Therefore, since test 3, run 101c, and test 4 showed no definite evidence of radial propagation of the boiling zone into the unblocked channels, it is concluded that radial boiling zone propagation is also unlikely in a 217-pin subassembly with a 6-channel blockage and with the same degree of boiling as produced in bundle 3B.

Two nonprototypicalities of bundle 3B must be discussed before the idealized extrapolation discussed above can be accepted. One nonprototypicality is the length of the unheated section downstream of the heated section. The short 76-mm (3-in.) unheated length in bundle 3B compared to the 1219-mm (48-in.) unheated length [in addition to the 305-mm (12-in.) axial blanket region] in an LMFBR subassembly leads to a lower frictional pressure drop downstream of the heated section in bundle 3B and therefore lower static pressure (sodium saturation temperature) downstream of the blockage; a similar bundle 3B test-section exit pressure and LMFBR argon cover gas pressure is thereby assumed. The resulting higher sodium saturation temperature immediately downstream of the blockage in a 217-pin LMFBR subassembly would lead to an even higher radial stability factor for boiling in a 6-channel blockage wake of a 217-pin bundle (see Table 4).

Another nonprototypicality in the 19-rod bundle 3B is the proximity of the duct wall to the 6-channel blockage, which results in a steeper radial temperature gradient in the subcooled channels near the duct wall than would occur in the same radial flow channels of a 217-pin assembly with a 6-channel blockage. However, it is important to note from Fig. 15 that the steepness of the radial temperature gradient between the wake boiling temperature and the adjacent subcooled region (approximately at single-phase bulk temperatures) is considered to be much greater for the 217-pin assembly than for the 19-rod assembly; this indicates that it is not the proximity of the duct wall but rather the bulk single-phase sodium temperature in the subcooled region that is the governing factor for radial boiling zone propagation when extrapolating 19-rod bundle results to 217-pin bundles with similar internal blockages. Thus, because of the higher bulk temperatures in bundle 3B (with greater likelihood of radial boiling zone propagation), the proximity of the duct wall is not considered a hindrance in extrapolating the 19-rod results. Furthermore, because of the difference in bulk temperatures between the 19-pin and 217-pin bundles, the 6-channel blockage

could be located anywhere within the 217-pin bundle (but at least two rows away from the duct wall, as in bundle 3B), and bundle 3B radial boiling propagation results could still be extrapolated to 217-pin bundles.

QUASI-STEADY-STATE BOILING WITH INERT-GAS INJECTION

Tests Conducted

Five experimental test runs, as shown in Table 5, were conducted to determine if inert-gas injection causes the local boiling downstream of a partial blockage to propagate radially into the unblocked channels. Since gas injection in two of the test runs (102b and 103a) was dubious because of sodium backed up in the gas injection line, two of the remaining three test runs (runs 102c and 103b) were chosen for analysis; these latter two tests included gas injection at two different rates. In addition, run 101f (without gas injection) was analyzed to compare boiling test runs with and without gas injection and is included in Table 5. All of the three test runs have similar test conditions, that is, 18 heaters operative, heater power of approximately 16.5 kW/m (5 kW/ft), and two flow coastdowns terminating in quasi-steady-state boiling periods of 10 to 15 sec. As a matter of consistency and because of the relatively long duration of boiling, the second low-flow period was chosen for detailed analysis; Figs. 17 to 19 show the responses of typical thermocouples downstream of the blockage and of the test-section inlet flowmeter.

Test Results

The responses of all thermocouples located between 330 mm (13.0 in.) and 584 mm (23.0 in.) from the start of the heated section were analyzed, and the results for the second quasi-steady-state boiling period of the three runs are presented in Table 6.

In Table 6, temperatures of the nearest surface in contact with sodium at a particular thermocouple location were calculated using the following assumptions: (1) for internal heater thermocouples (those with R prefix), it was assumed that the heat flux in the heater cladding travels radially

Table 5. Bundle 3B quasi-steady-state boiling experiments with inert-gas injection — test series 8 (bundle 3B), test 3[a]

Initial test-section flow[b] = 1.4 liters/sec (22 gpm)

Run	Date	Number of heaters operative	Average uniform heater power [kW/m (kW/ft)]	Average inlet temperature [°C (°F)]	Average flow during quasi-steady-state boiling periods (gpm)	Gas injection rate [g/hr (lb_m/hr)]	Duration of quasi-steady-state boiling periods (sec)
102a	4-9-75	19[c]	16.5 (5.0)	570 (1060)	7.0	1.4 (0.003)	10
102b	4-9-75	18	16.5 (5.0)	515 (960)	6.5, 5.5	1.4 (0.003)[d]	5, 10
102c[e]	4-9-75	18	16.1 (4.9)	513 (955)	5.2, 5.3	1.4 (0.003)	13, 11
103a	4-9-75	18	16.5 (5.0)	515 (960)	5.5, 5.5	5.4 (0.012)[d]	5, 10
103b[e]	4-9-75	18	16.3 (5.0)	513 (955)	5.2, 5.4	5.4 (0.012)	10, 15
101f[e,f]	4-9-75	18	16.1 (4.9)	515 (960)	6.4, 6.1	None	6, 14

[a] Conversion factors: 1 gpm = 0.063 liter/sec; 1 fps = 0.305 m/sec.

[b] 100% Fast Flux Test Facility (FFTF) flow (corresponding to a velocity of 24 fps) = 54 gpm in bundle 3B.

[c] Heater 7 electrical circuit failed after 10 sec of sodium boiling.

[d] Gas injection line was accidentally blocked during these runs; probably no gas was injected into bundle.

[e] Chosen for analysis.

[f] This run without gas injection is listed for the purpose of comparison, as discussed in the text.

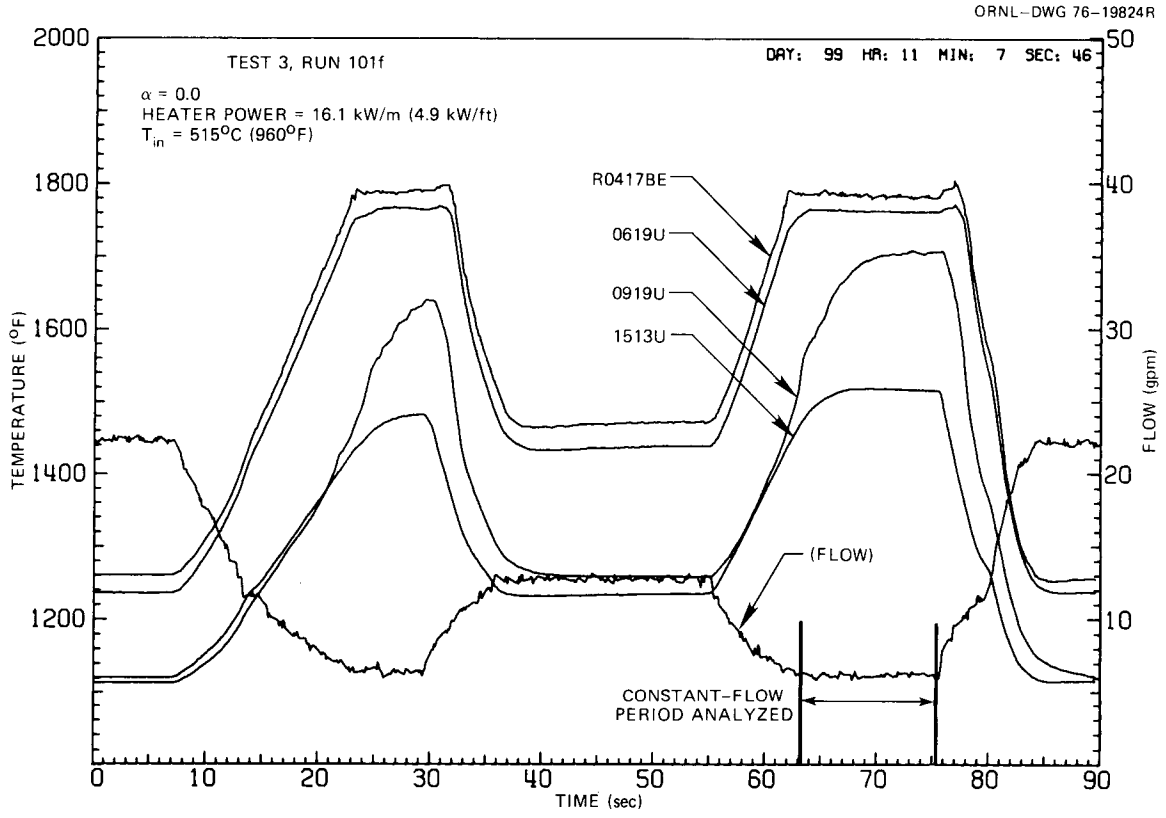

Fig. 17. Selected thermocouple responses and test-section inlet flowmeter response for test series 8 (bundle 3B), test 3, run 101f [no gas injection (void fraction α = 0.01)]. Thermocouple R0417BE is a grounded heater 4 internal thermocouple located 422 mm (16.63 in.) downstream from the start of the heated section, and thermocouples 0619U, 0919U, and 1513U are centrally located, ungrounded wire-wrap thermocouples at 483 mm (19.0 in.) on heater 6, at 483 mm (19.0 in.) on heater 9, and at 330 mm (13.0 in.) on heater 15, respectively [1 gpm = 0.063 liter/sec; °C = 5/9 (°F - 32)].

outward in a uniform manner around the heater circumference; (2) for thermocouples in the center of wire wraps (those with the suffix U), it was assumed that the temperature drop from the center of the wire wrap to the wire surface was one-half the measured temperature drop across one entire wire wrap at the 431-mm (17.0-in.) location (see measured temperatures of thermocouples 0217A and 0217B in Table 6); and (3) temperatures of wire-wrap thermocouples at the unheated 584-mm (23.0-in.) level as well as on the failed heater 7 (thermocouple 0719A) were assumed to be the same as those on the wire-wrap surface, since there is very little radial heat conduction in the unheated portion of the rods at the end of the constant-flow period

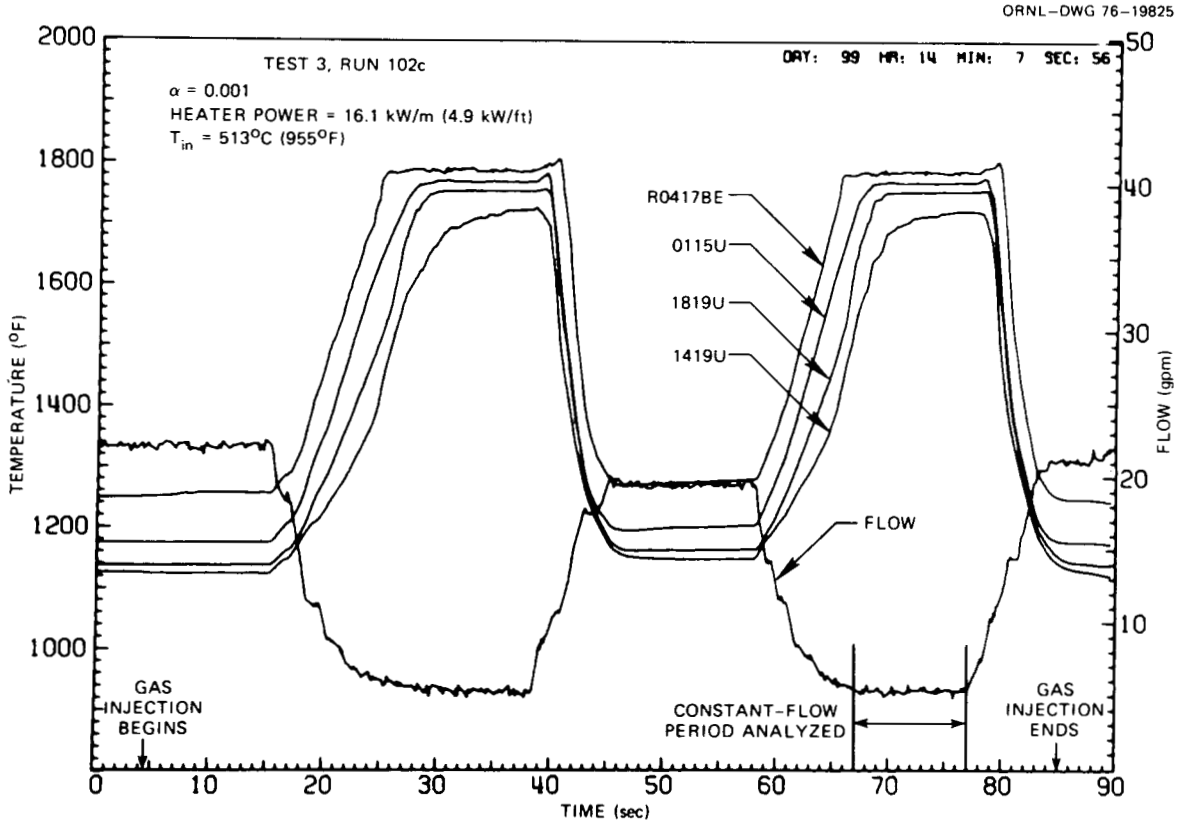

Fig. 18. Selected thermocouple responses and test-section inlet flowmeter response for test series 8 (bundle 3B), test 3, run 102c (void fraction α = 0.001). Thermocouple R0417BE is a grounded heater 4 internal thermocouple located 422 mm (16.63 in.) downstream from the start of the heated section, and thermocouple 0115U, 1819U, and 1419U are centrally located ungrounded wire-wrap thermocouples at 381 mm (15.0 in.) on heater 1, at 483 mm (19.0 in.) on heater 18, and at 483 mm (19.0 in.) on heater 14, respectively [1 gpm = 0.063 liter/sec; °C = 5/9 (°F - 32).]

analyzed. The latter argument is also applicable to the internal heater thermocouples in failed heater 7.

Vapor generation during the quasi-steady-state boiling period in question was established from the thermocouple responses in the same way as was previously described for the runs without gas injection.

Void fraction values shown in Table 6 were calculated at the start of the heated section by assuming that there was no slip between the two phases (homogeneous flow), that thermodynamic equilibrium exists between the two phases, and that argon behaves like a perfect gas. Thus, the void fraction

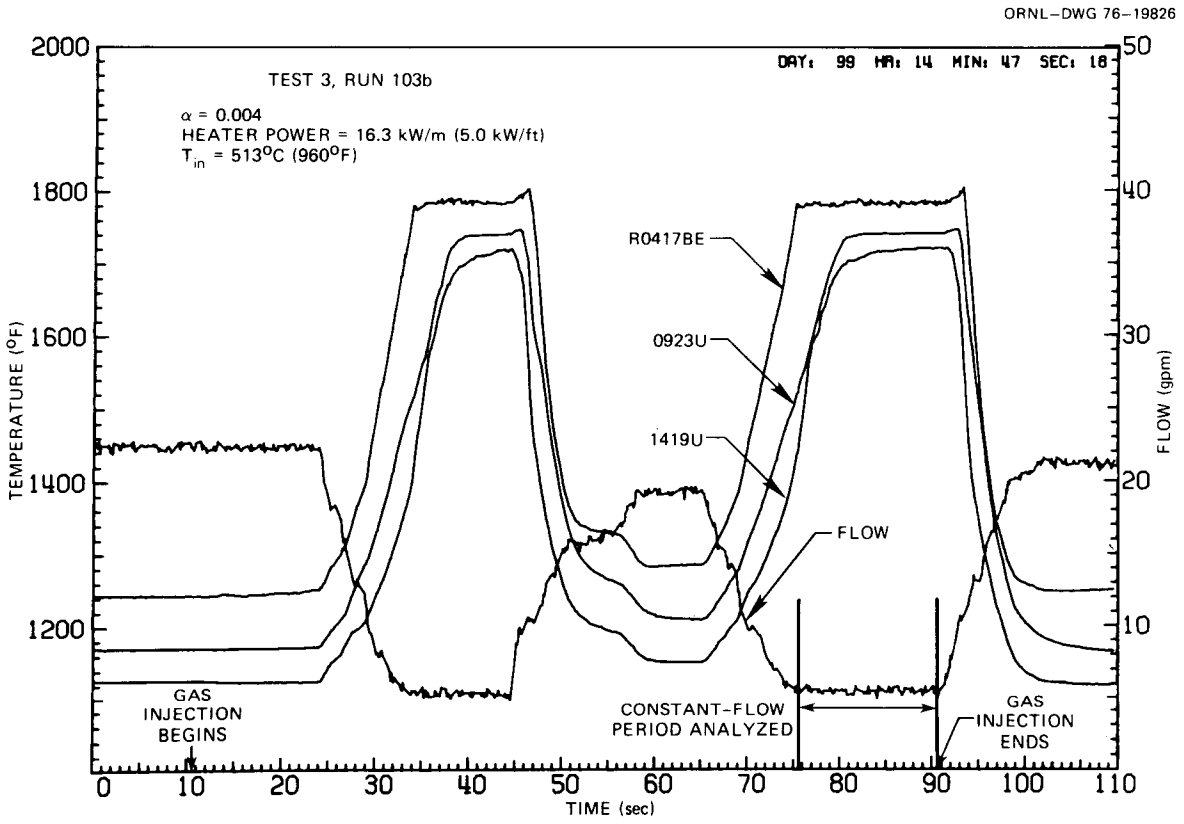

Fig. 19. Selected thermocouple responses and test-section inlet flowmeter response for test series 8 (bundle 3B), test 3, run 103b (void fraction α = 0.004). Thermocouple R0417BE is a grounded heater 4 internal thermocouple located 422 mm (16.63 in.) downstream from the start of the heated section, and thermocouples 0923U and 1419U are centrally located, ungrounded wire-wrap thermocouples at 584 mm (23.0 in.) on heater 9 and at 483 mm (19.0 in.) on heater 14, respectively [1 gpm = 0.063 liter/sec; °C = 5/9 (°F - 32)].

(α) of argon (Ar) in sodium (Na) is defined as

$$\alpha\left(\begin{matrix}\text{at start of}\\ \text{heated section}\end{matrix}\right) = \frac{C_{Ar}}{C_{Ar} + C_{Na}} = \frac{W_{Ar}/\rho_{Ar}}{(W_{Ar}/\rho_{Ar}) + W^{l}_{Na}} ,$$

where

C = cross-sectional bundle flow area (ft^2),

W = mass flow (lb_m/hr),

W^l = mass flow (gpm),

ρ = density (lb_m/ft^3) (calculated from the perfect gas law at sodium pressure and temperature).

Table 6. Results of bundle 3B quasi-steady-state boiling tests (with gas injection)

Distance from start of heated section [mm (in.)]	Thermocouple[a]	Test 3, run 101f Test conditions: Flow: 0.39 liter/sec (6.1 gpm) Heater power: 16.0 kW/m (4.9 kW/ft) Inlet temperature: 516°C (960°F) Quasi-steady-state boiling period: 63.0–75.5 sec Argon gas void fraction: 0.0				Test 3, run 102c Test conditions: Flow: 0.33 liter/sec (5.3 gpm) Heater power: 16.0 kW/m (4.9 kW/ft) Inlet temperature: 513°C (955°F) Quasi-steady-state boiling period: 67.0–77.0 sec Argon gas void fraction: 0.001				Test 3, run 103b Test conditions: Flow: 0.34 liter/sec (5.4 gpm) Heater power: 16.4 kW/m (5.0 kW/ft) Inlet temperature: 513°C (955°F) Quasi-steady-state boiling period: 75.2–90.5 sec Argon gas void fraction: 0.004			
		Measured temperature at end of period [°C (°F)]	Estimated surface temperature at end of period [°C (°F)]	Evidence of vapor generation during period	Time of temperature stabilization[b] for period (sec)	Measured temperature at end of period [°C (°F)]	Estimated surface temperature at end of period [°C (°F)]	Evidence of vapor generation during period	Time of temperature stabilization for period (sec)	Measured temperature at end of period [°C (°F)]	Estimated surface temperature at end of period [°C (°F)]	Evidence of vapor generation during period	Time of temperature stabilization for period (sec)
Blocked region													
381 (15.0)	0115U	960 (1760)	957 (1755)	?	66.5	963 (1765)	960 (1760)	Yes	68.1	963 (1765)	960 (1760)	Yes	78.0
381 (15.0)	0315U	957 (1755)	954 (1750)	?	66.3	957 (1755)	954 (1750)	Yes	67.6	957 (1755)	954 (1750)	Yes	76.9
390 (15.35)	R0615AB	982 (1800)	968 (1775)	Yes	65.3	985 (1805)	971 (1780)	Yes	68.0	985 (1805)	971 (1780)	Yes	78.3
391 (15.38)	R0215AD	960 (1760)	946 (1735)		66.5	985 (1805)	971 (1780)	Yes	70.7	985 (1805)	971 (1780)	Yes	80.2
396 (15.60)	R0515BC	966 (1770)	952 (1745)	Yes	65.2	966 (1770)	952 (1745)	Yes	67.6	963 (1765)	949 (1740)	Yes	76.9
397 (15.63)	R0215CD	982 (1800)	968 (1775)	Yes	64.4	980 (1790)	963 (1765)	Yes	66.8	979 (1795)	966 (1770)	Yes	76.9
403 (15.85)	R0616CD	971 (1780)	957 (1755)	Yes	64.2	971 (1780)	957 (1755)	Yes	66.7	971 (1780)	957 (1755)	Yes	76.8
409 (16.10)	R0616DE	971 (1780)	957 (1755)	Yes	65.4	971 (1780)	957 (1755)	Yes	67.6	974 (1785)	960 (1760)	Yes	77.0
410 (16.13)	R0416AB	971 (1780)	957 (1755)	Yes	63.8	971 (1780)	957 (1755)	Yes	66.3	971 (1780)	957 (1755)	Yes	77.6
416 (16.38)	R0716BC	938 (1720)	924 (1720)	Yes	66.8	938 (1720)	924 (1695)	Yes	70.8	unreliable			
416 (16.38)	R0416BC	966 (1770)	952 (1745)	Yes	61.9	966 (1770)	952 (1745)	Yes	66.9	966 (1770)	952 (1745)	Yes	76.3
416 (16.38)	R0516BC	991 (1815)	980 (1790)	Yes	62.8	991 (1815)	980 (1790)	Yes	66.3	993 (1820)	979 (1795)	Yes	76.3
422 (16.63)	R0417BE	971 (1780)	957 (1755)	Yes	61.7	971 (1780)	957 (1755)	Yes	65.5	971 (1780)	957 (1755)	Yes	75.2
422 (16.63)	R0517CD	993 (1820)	979 (1795)	Yes	63.2	991 (1815)	980 (1790)	Yes	67.8	993 (1820)	979 (1795)	Yes	78.2
422 (16.63)	R0717BE	954 (1750)	941 (1725)	?	66.3	954 (1750)	941 (1725)	Yes	70.7	unreliable			
432 (17.0)	0117U	957 (1755)	954 (1750)	Yes	62.5	957 (1755)	954 (1750)	Yes	65.8	957 (1755)	954 (1750)	Yes	75.5
432 (17.0)	0217A	963 (1765)	957 (1755)	Yes	63.8	960 (1760)	957 (1755)	Yes	66.5	960 (1760)	957 (1755)	Yes	76.3
432 (17.0)	0217B	957 (1755)	954 (1750)	Yes	62.8	957 (1755)	957 (1755)	Yes	66.3	957 (1755)	957 (1755)	Yes	75.7
483 (19.0)	0619U	960 (1760)	957 (1755)	Yes	63.2	960 (1760)	957 (1755)	Yes	66.3	957 (1755)	954 (1750)	Yes	76.3
483 (19.0)	0719A	957 (1755)	952 (1755)	Yes	63.8	954 (1750)	952 (1750)	Yes	66.8	957 (1755)	957 (1755)	Yes	76.4
533 (21.0)	0521U	957 (1755)	954 (1750)	Yes	62.6	957 (1755)	954 (1750)	Yes	65.7	957 (1755)	954 (1750)	Yes	75.3
533 (21.0)	0621U	957 (1755)	954 (1750)	Yes	62.6	957 (1755)	954 (1750)	Yes	65.5	957 (1755)	954 (1750)	Yes	75.4
584 (23.0)	0423U	954 (1750)	954 (1750)	?	70.1	952 (1745)	952 (1745)	Yes	72.6	952 (1745)	952 (1745)	Yes	81.3
Unblocked region													
330 (13.0)	0313U	899 (1650)	896 (1645)	No	66.3	957 (1755)	954 (1750)	No	71.3	954 (1750)	952 (1745)	No	82.8
330 (13.0)	0413U	902 (1655)	899 (1650)	No	65.8	960 (1760)	957 (1755)	No	70.8	960 (1760)	957 (1755)	No	82.6
330 (13.0)	1113U	877 (1610)	874 (1605)	No	66.3	927 (1700)	924 (1695)	No	71.9	921 (1690)	918 (1685)	No	82.9
330 (13.0)	1513U	824 (1515)	821 (1510)	No	66.4	888 (1630)	885 (1625)	No	71.6	882 (1620)	871 (1615)	No	82.8
330 (13.0)	1713U	746 (1375)	743 (1370)	No	68.8	777 (1430)	774 (1425)	No	74.2	774 (1425)	771 (1420)	No	83.8
381 (15.0)	0815A	891 (1635)	893 (1640)	No	67.6	935 (1715)	943 (1730)	No	73.8	935 (1715)	941 (1725)	No	85.1
381 (15.0)	0815B	893 (1640)	893 (1640)	No	67.6	943 (1730)	943 (1730)	No	73.8	941 (1725)	941 (1725)	No	85.1
381 (15.0)	1015U	927 (1700)	924 (1695)	?	66.6	954 (1750)	952 (1745)	Yes	69.4	954 (1750)	952 (1745)	Yes	80.4
381 (15.0)	1515U	807 (1485)	804 (1480)	No	67.7	874 (1605)	871 (1600)	No	72.8	874 (1605)	871 (1600)	No	85.1
381 (15.0)	1915U	866 (1590)	863 (1585)	No	67.6	929 (1705)	927 (1700)	No	74.3	924 (1695)	921 (1690)	No	84.3
432 (17.0)	1017U	916 (1680)	913 (1675)	?	65.2	957 (1755)	954 (1750)	Yes	74.0	957 (1755)	954 (1750)	Yes	83.1
432 (17.0)	1117U	891 (1635)	888 (1630)	No	70.1	929 (1705)	927 (1700)	No	75.1	924 (1695)	921 (1690)	Yes	83.9
432 (17.0)	1817U	878 (1615)	877 (1610)	No	68.8	938 (1720)	935 (1715)	Yes	74.0	935 (1715)	932 (1710)	Yes	83.2
432 (17.0)	1917U	935 (1715)	932 (1710)	?	67.6	957 (1755)	954 (1750)	Yes	71.7	954 (1750)	952 (1745)	No	82.8
447 (17.59)	R1418AB	843 (1550)	827 (1520)	No	66.4	907 (1665)	893 (1640)	No	72.6	913 (1675)	899 (1650)	No	88.8
447 (17.59)	R1418BC	860 (1580)	849 (1560)	No	66.3	916 (1680)	902 (1655)	No	72.6	927 (1700)	913 (1675)	No	90.1
483 (19.0)	0919U	929 (1705)	927 (1700)	No	70.4	957 (1755)	954 (1750)	Yes	74.2	957 (1755)	954 (1750)	Yes	85.1
483 (19.0)	1419U	916 (1680)	913 (1675)	No	68.9	935 (1715)	932 (1710)	Yes	74.0	938 (1720)	935 (1715)	Yes	83.9
483 (19.0)	1819U	946 (1735)	943 (1730)	?	67.0	954 (1750)	952 (1745)	Yes	69.0	954 (1750)	952 (1745)	Yes	78.8
584 (23.0)	0923U	949 (1740)	949 (1740)	?	70.1	949 (1740)	949 (1740)	Yes	70.8	949 (1740)	949 (1740)	Yes	81.3
584 (23.0)	1423U	938 (1720)	938 (1720)	?	71.7	952 (1745)	952 (1745)	Yes	73.1	952 (1745)	952 (1745)	Yes	82.6

[a] Numbers of wire-wrap thermocouples consist of four digits followed by a single letter (e.g., 0315U, 0217A, and 0217B). The first two digits give the heater number (see Fig. 10) adjacent to the wire wrap, the second two digits give the axial location downstream of the start of the heated section, and the single letter stands for the physical location inside the wire wrap (i.e., U indicates an ungrounded type in the center of the wire wrap, A indicates a grounded thermocouple adjacent to the heater, and B indicates a grounded type adjacent to sodium). Numbers of grounded heater internal thermocouples start with the letter R and are followed by four digits for the heater number and the axial location downstream from the start of the heated section; the final two letters indicate the thermal elements which form the thermocouple junction.

[b] Temperature stabilization is defined as being reached whenever 99% of temperature rise is reached during flow coastdown period.

The test results listed in Table 6 are graphically presented for each of the three runs in Figs. 20 to 22. Also included is the single-phase axial sodium bulk temperature (assuming no blockage) and an estimated sodium saturation temperature in the unblocked channels. The saturation temperature shown in the two-phase region downstream of the blockage was determined in the same way as it was for the cases without gas injection; that is, the static axial pressure profile was first determined at those positions where single-phase flow definitely prevailed (upstream of the blockage and downstream of the attemperator near the bundle outlet); the remaining axial static pressures in the two-phase region were then estimated by linear interpolation and finally converted to the sodium saturation temperature.

Discussion of Test Results

The experimental results presented in Table 6 and Figs. 20 to 22 basically indicate the following observations for bundle 3B local boiling with gas injection:

1. Six of the nine thermocouples in the unblocked channels from 50.8 mm (2.0 in.) to 101.6 mm (4.0 in.) downstream of the blockage show evidence of sodium vapor during the quasi-steady-state boiling periods with gas injection (see Figs. 21 and 22). Figure 20 ($\alpha = 0$), on the other hand, shows that none of these thermocouples indicates sodium vapor in its vicinity. This difference can be attributed either to radial propagation of the local boiling zone (caused by inert-gas injection) or to the higher sodium bulk temperature in the gas injection runs (caused by larger power-to-flow ratios). It is not evident that these effects may be separated from the data taken. However, it is noted that two thermocouples (1817U and 1419U) in the unblocked channels at 50.8 mm (2.0 in.) and 101.6 mm (4.0 in.) downstream of the blockage indicate sodium vapor at approximately 20°C (40°F) below the estimated saturation temperature (see Figs. 21 and 22). Since the same two thermocouples do not show evidence of vapor in the run without gas injection (Fig. 20), it is believed that inert-gas bubbles at these two thermocouple locations do influence vapor production or propagation.

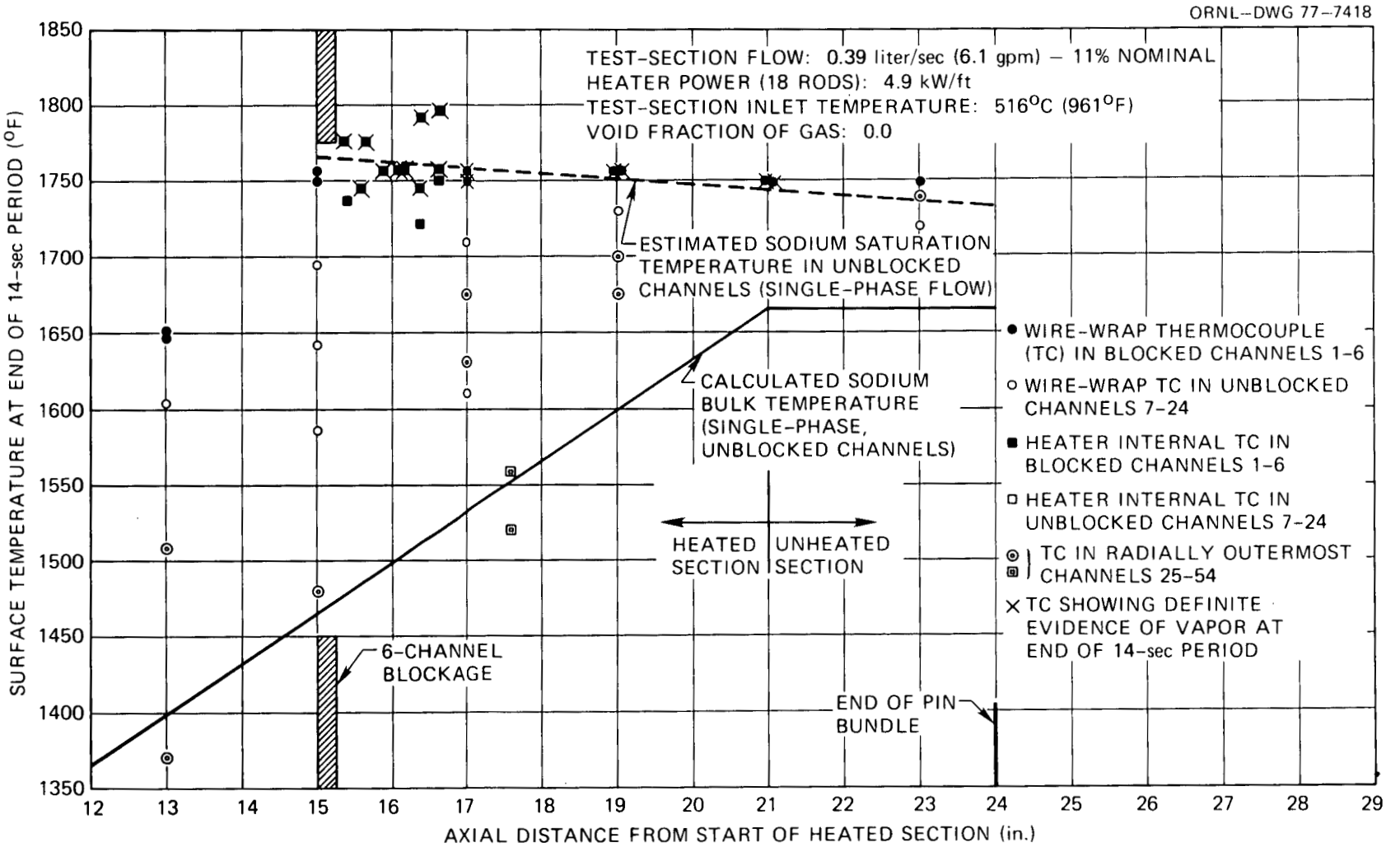

Fig. 20. Experimental temperatures in vicinity of blockage at end of 14-sec period in test 3, run 101f (1 in. = 25.4 mm).

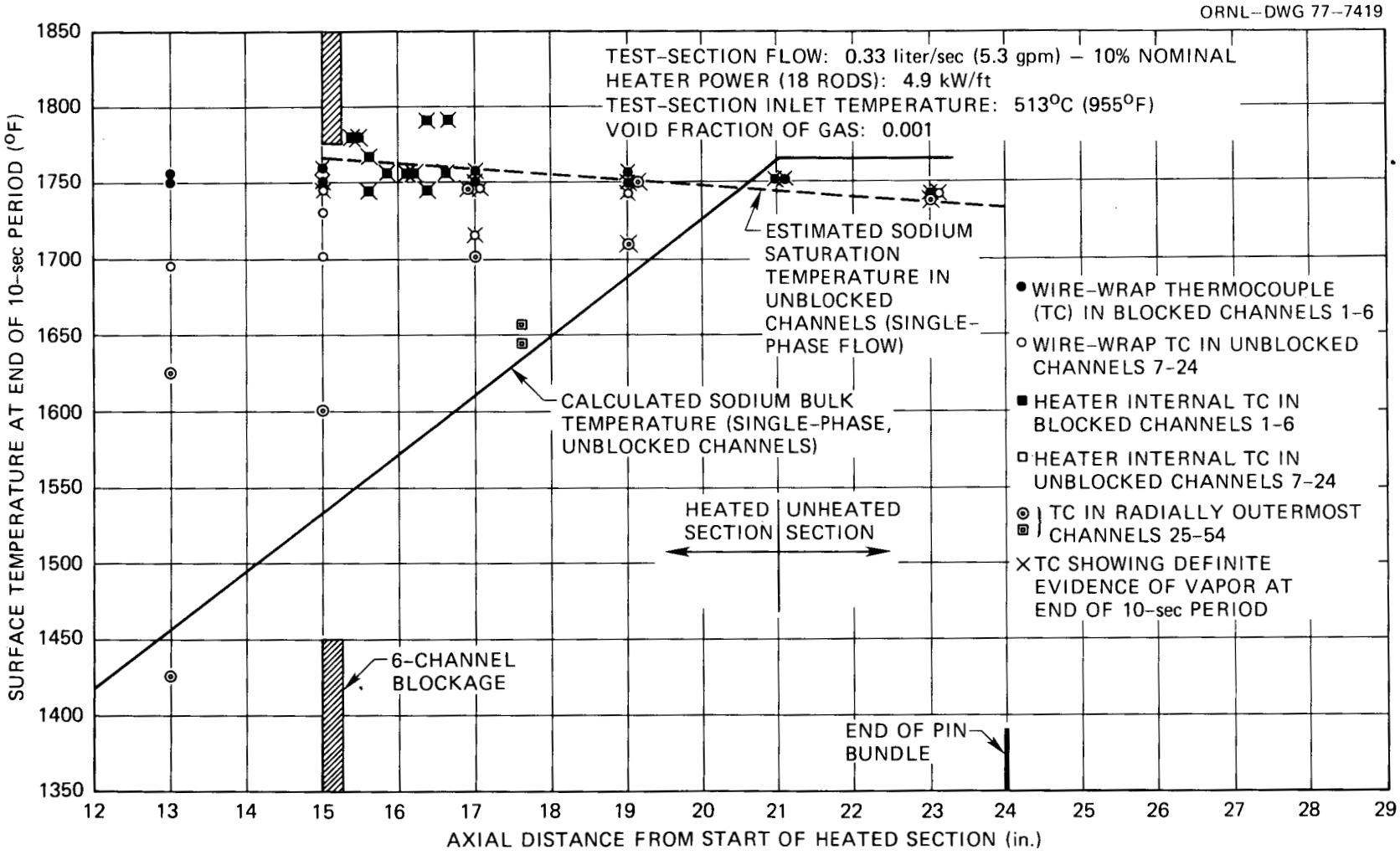

Fig. 21. Experimental temperatures in vicinity of blockage at end of 10-sec period in test 3, run 102c (1 in. = 25.4 mm).

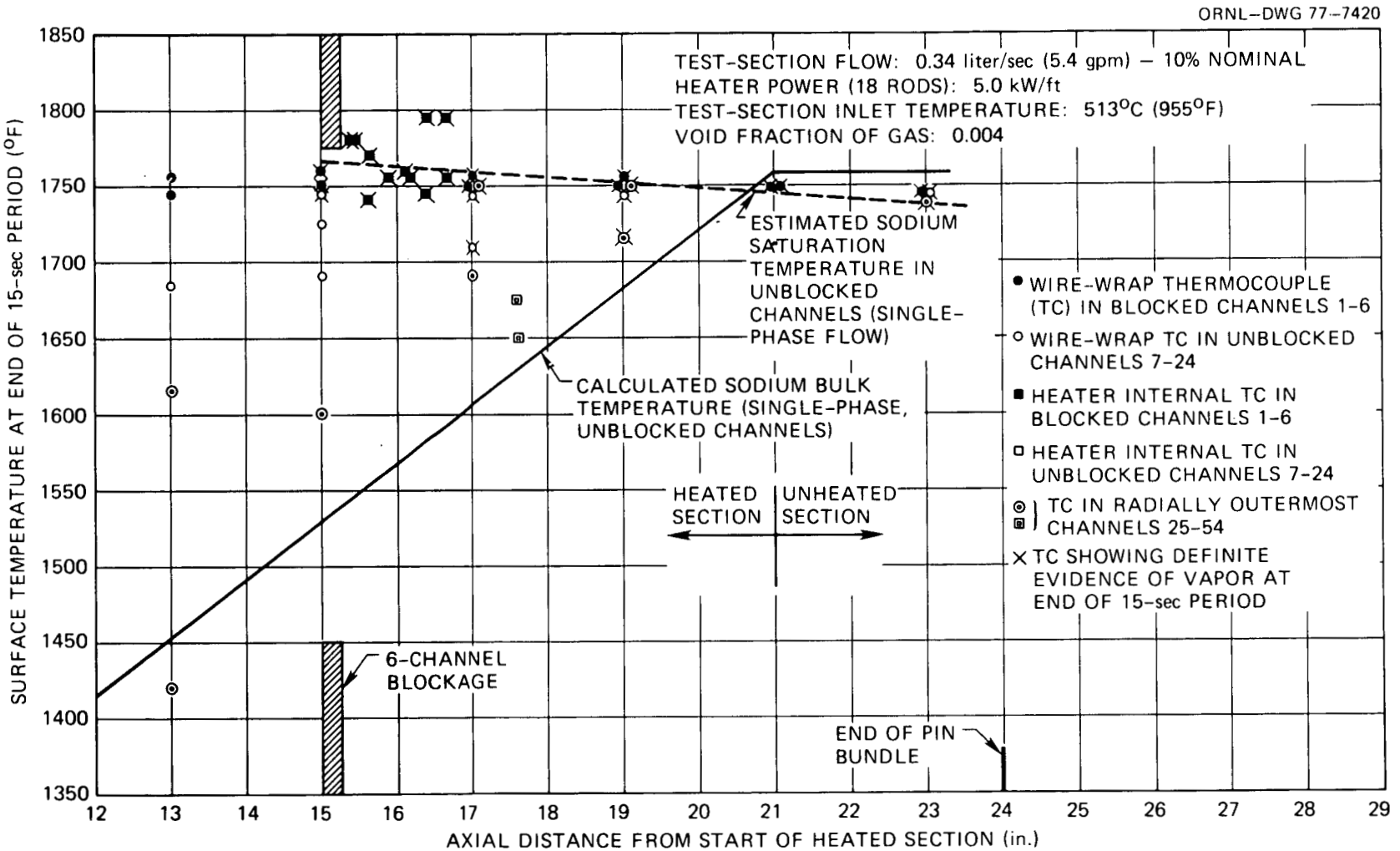

Fig. 22. Experimental temperatures in vicinity of blockage at end of 15-sec period in test 3, run 103b (1 in. = 25.4 mm).

2. The two runs with gas injection show the same number of thermocouples with evidence of sodium vapor at essentially the same location. This indicates that increasing the void fraction of inert gas from 0.001 to 0.004 while keeping flow and heater power constant does not affect the extent of the local boiling zone. There appears to be an upper limit of gas accumulation in the blockage wake beyond which additional gas injection does not have any influence on the local boiling zone.

3. All temperatures in the unblocked channels had stabilized 2 sec prior to the end of the 10-sec boiling period when $\alpha = 0.001$, and all except one temperature had also stabilized 2 sec prior to the end of the 15-sec boiling period when $\alpha = 0.004$. The one temperature which had not stabilized [thermocouple R1418BC at the 460-mm (18.0-in.) level on heater 14] showed a very low rate of temperature change at the end of the period analyzed. These results indicate that stable flow conditions (stable bundle-cooling capability) had been maintained at the end of the quasi-steady-state boiling periods with gas injection.

4. None of the thermocouples indicating sodium vapor conditions increased steeply above 982°C (1800°F) during the quasi-steady-state boiling periods. Local cladding dryout due to vapor and/or inert-gas blanketing (loss of liquid film) is thereby discounted.

Conclusions

1. Bundle 3B results with gas injection show some evidence that inert-gas injection ($\alpha = 0.001$ and $\alpha = 0.004$) is partially responsible for the presence of vapor in the unblocked channels surrounding a 6-channel blockage wake, although boiling across the entire bundle cross section did not occur.

2. Increasing the void fraction of inert gas from 0.001 to 0.004 does not essentially influence the extent of the local boiling zone.

3. Stable temperature conditions throughout the bundle are in evidence at the end of the quasi-steady-state boiling periods with gas injection.

4. There was no evidence of cladding dryout (loss of liquid film) in the local boiling zone during quasi-steady-state boiling.

SINGLE-PHASE STEADY-STATE TESTS WITH ARGON GAS INJECTION

Purpose

The argon gas injection system was used with bundle 3B to investigate the effect of inert gas on temperatures downstream of the blockage during single-phase steady-state tests. Partially blocked LMFBR subassemblies may accumulate inert gas downstream of the blockage and increase the temperature there; this inert gas may originate either from being entrained in the sodium or from fission gas leaking from a fuel pin upstream of the blockage.

In particular, an effort has been made to determine trends of maximum temperature increase as a function of the flow-power combination and of inert void fraction. Two different rates of gas injection were used at a specified flow-power combination.

In addition, by observing the thermocouple responses in the blockage wake after gas injection was stopped, it was thought possible to determine the length of time necessary for accumulated gas to be removed from the blockage and for pre-gas-injection conditions to be reestablished. An answer to this latter point would give an indication of how long the effect of a temporary increase in inert-gas void fraction would produce an effect downstream of a partial blockage, where temperature conditions would be most severe from the standpoint of cladding structural integrity.

Tests Conducted

Table 7 gives the test conditions for each of the ten experimental runs. Also shown is the calculated void fraction at the beginning of the heated section [381 mm (15 in.) upstream of the blockage]; the void fraction was defined earlier in this report.

The procedure used to obtain experimental data for each run was as follows: (1) steady-state conditions of sodium flow, heater power, and inlet temperature were initially established; (2) the data-acquisition system, which recorded all instrument signals every 0.1 sec, was then activated; (3) several seconds later, argon gas was injected for a specified time period at a specified flow; and (4) after gas injection was terminated, data acquisition was continued for up to 3 min.

Table 7. Bundle 3B steady-state nonboiling experiments with gas injection — test series 8 (bundle 3B), test 2, all 19 heaters powered

Run No.	Date	Average Uniform heater power [kW/m (kW/ft)]	Average sodium flow[a] [liters/sec (gpm)]	Average inlet temperature [°C (°F)]	Gas injection rate [g/hr (lb_m hr)]	Duration of gas injection (sec)	α, calculated void fraction at beginning of heated section[b]
101	4-3-75	3.2 (9.8)	3.47 (55.0)	456 (853)	3.5 (0.0076)	61	0.00009
102	4-3-75	3.2 (9.8)	3.46 (54.8)	457 (855)	5.4 (0.012)	61	0.00015
103	4-2-75	2.0 (6.1)	1.23 (19.5)	322 (611)	1.4 (0.003)	62	0.00016
104	4-2-75	2.0 (6.1)	1.23 (19.5)	322 (611)	5.4 (0.012)	62	0.00065
105	4-3-75	1.4 (4.3)	0.979 (15.5)	321 (608)	1.4 (0.003)	92	0.00022
106	4-3-75	1.4 (4.3)	0.979 (15.5)	319 (607)	5.4 (0.012)	90	0.00087
107	4-3-75	0.97 (3.0)	0.657 (10.4)	301 (547)	1.4 (0.003)	62	0.00035
108	4-3-75	0.97 (3.0)	0.651 (10.3)	298 (569)	5.4 (0.012)	60	0.00135
109	4-4-75	0.49 (1.5)	0.32 (5.0)	303 (578)	1.4 (0.003)	61	0.00078
110	4-4-75	0.49 (1.5)	0.27 (4.3)	282 (540)	5.4 (0.012)	61	0.00354

[a] 100% Fast Flux Test Facility (FFTF) flow (corresponding to a velocity of 24 fps) = 54 gpm in bundle 3B (1 gpm = 0.063 liter/sec, 1 fps = 0.305 m/sec).

[b] Void fraction calculation made with the following assumptions: 1. Sodium velocity = argon bubble velocity (slip ratio = 1). 2. Thermodynamic equilibrium between sodium liquid and argon bubbles: ($T_{Na} = T_{Ar}$, $P_{Na} = P_{Ar}$). 3. Argon gas behaves like a perfect gas.

Test Results

The responses of all thermocouples were studied for each test run; Table 8 gives the results of this analysis for the blockage wake. The peak temperature and the average temperature showing the most pronounced increase during gas injection are compared to the steady-state temperatures before gas was injected. In addition, average residual temperatures were obtained 30 sec after gas injection was stopped and at the end of each test run; these temperatures are compared to the steady-state temperatures. The steady-state temperature for a particular thermocouple was taken as the average temperature recorded during the first second of the test run (except for run 105 where the first temperature reading was used because the start of gas injection coincided with the start of data acquisition).

Discussion of Test Results

Table 8 does not show any obvious relationship between the maximum temperature increase due to gas injection and the flow-power combination of the void fraction.

The maximum temperature increase and the average temperature increase over the pre-gas-injection temperature are largest during run 104 (α = 0.00065), being 39°C (70°F) and 35°C (63°F), respectively, at a steady-state thermocouple temperature of 591°C (1096°F). The thermocouple exhibiting this increase is RO116CD, a grounded internal heater thermocouple located on heater 1 (central heater) 16 mm (0.63 in.) downstream of the blockage; the thermocouple response is shown in Fig. 23. Previous tests without gas injection using the same bundle (FFM bundle 3A) had established that sodium temperature increases due to six-channel central blockages are generally no more than 120°C (220°F) above steady-state sodium temperatures in similar unblocked bundles.[15] Combining the peak temperature increase due to both inert-gas injection (at α = 0.00065) and a six-channel central blockage results in a maximum sodium temperature increase in bundle 3B of no more than 160°C (290°F). Although such a maximum temperature increase would not endanger reactor safety from the standpoint of reaching sodium saturation temperatures of approximately 930°C (1700°F), it is interesting that such a small void fraction of argon gas accounts for one-fourth of the

Table 8. Test results for bundle 3B, test 2, runs 101 to 110[a]

Run No.	Void fraction	Flow (gpm)	Power (kW/rod)	Thermocouples[b] with most pronounced temperature increase	Axial position of thermocouple downstream of blockage [mm (in.)]	Steady-state temperature before gas injection (°C)	Maximum ΔT increase during gas injection (°C)	Average ΔT increase during gas injection[c] (°C)	Residual ΔT 30 sec after gas injection ends (°C)	Residual ΔT at end of run (°C) @ number of seconds after gas injection ends
101	0.00009	55.0	17.1	R0116DE	22 (0.88)	632	4	0	0	
				R0116CD	16 (0.63)	642	2	0	0	
102	0.00015	54.8	17.1	R0116DE	22 (0.88)	633	3	1	2	1.5 @ 25
				R0116CD	16 (0.63)	641	4	1	1	1.5 @ 25
103	0.00016	19.5	10.7	R0615BC	10 (0.38)	577	15	7	8	6 @ 165
				R0116DE	22 (0.88)	577	11	3	3	0 @ 165
				R0116CD	16 (0.63)	590	15	11	13	1 @ 165
				0217B	51 (2.0)	517	7	7	6	0 @ 165
104	0.00065	19.5	10.7	R0615AB	9 (0.35)	582	23	7	11	3 @ 196
				R0615BC	10 (0.38)	583	23	5	18	4 @ 196
				R0116DE	22 (0.88)	582	18	15	12	15 @ 196
				R0116CD	16 (0.63)	591	39	35	31	29 @ 196
				0217B	51 (2.0)	517	9	7	6	5 @ 196
105	0.00022	15.5	7.6	R0615AB	9 (0.35)	538	9	8	8	8 @ 66
				R0615BC	10 (0.38)	541	11.5	6	6	5 @ 66
				R0116CD	16 (0.63)	556	12	11	10	11 @ 66
106	0.00087	15.5	7.6	R0615AB	9 (0.35)	540	10.5	7	8	8 @ 78
				R0516BC	35 (1.38)	539	8	4	5	5 @ 78
				R0116CD	41 (1.63)	556	16.5	12	8	8 @ 78
				R0517CD	41 (1.63)	542	7	4	5	5 @ 78
107	0.00035	10.4	5.2	R0116CD	16 (0.63)	522	1	0	0	-1 @ 63
				0919U	102 (4.0)	425	4.5	0	0	-1 @ 63
				0923U	203 (8.0)	436	4.5	0	0	-1 @ 63
108	0.00135	10.3	5.2	R0116CD	16 (0.63)	519	0.5	-1	0	0 @ 46
				0919U	102 (4.0)	423	5	1	0	0 @ 46
				0923U	203 (8.0)	434	5	1	0	0 @ 46
109[d]	0.00078	5.0	2.6							
110	0.00354	4.3	2.6	R0115AD	10 (0.38)	506	6.5	0	1	1 @ 47
				R0116CD	16 (0.63)	529	1	-3	-1	-1 @ 47
				R0417BE	41 (1.63)	516	7	-2	1	1 @ 47
				R0717BE	41 (1.63)	509	8	-2	0	0 @ 47
				0923U	203 (8.0)	476	5.5	0	1	1 @ 47

[a] Conversion factor: 1 gpm = 0.063 liter/sec.

[b] See footnote to Table 6 for explanation of thermocouple numbering system.

[c] After initial transient effect.

[d] An unplanned 4% inlet temperature decrease and an unplanned 15% test-section flow decrease during this test run make the results incomparable with those of the other test runs.

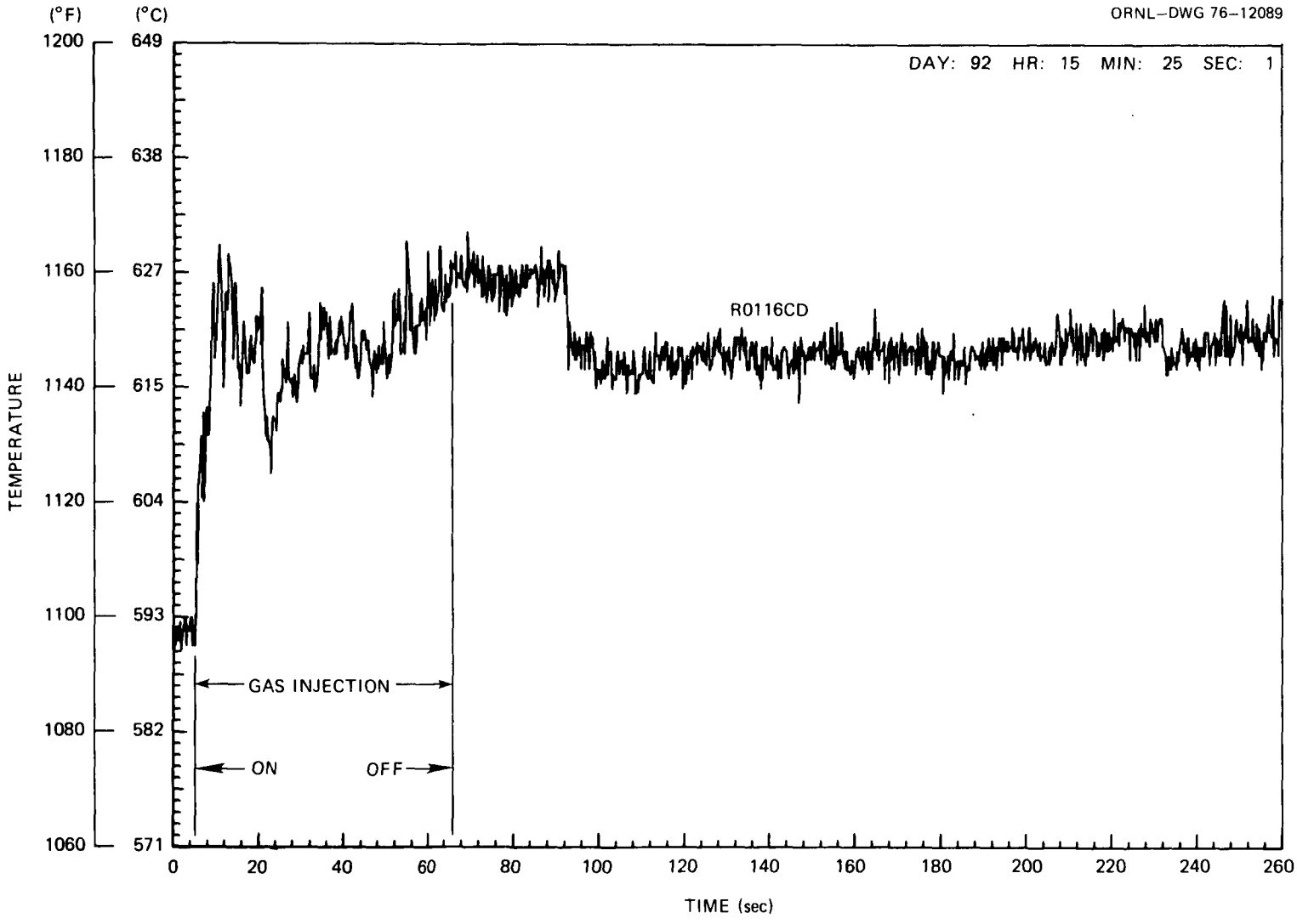

Fig. 23. Response of internal heater thermocouple R0116CD during test series 8, test 2, run 104, α = 0.00065. R0116CD is located on heater 1, 15.63 in. downstream from the start of the heated section and 0.63 in. downstream of the blockage (see Fig. 10).

combined temperature increase due to both gas injection and the six-channel central blockage.

Residual temperature increases in this discussion refer to the temperature increases (over pre-gas-injection steady-state temperatures) experienced by the thermocouples downstream of the blockage after termination of gas injection. The increases are a measure of the time required for gas accumulated in the blockage wake zone to be flushed out and thus give an indication of how long the effects of gas injection influence temperatures in the wake. An examination of the most pronounced residual temperature increases (runs 103 through 106 in Table 8) reveals that although some thermocouples (in run 104) show that most of the residual temperature increase has disappeared 193 sec after gas injection ends, others (RO116CD in run 104 and run 105) show no significant decrease in residual temperature increase even 193 sec after the end of gas injection. However, in comparing the steady-state pre-gas-injection temperature of RO116CD in runs 105 and 106 (same test conditions), it is noteworthy that any temperature increases due to gas injection in run 105 had disappeared at the start of run 106 (see Figs. 24 and 25). Since the time difference between these two runs was 19 min and 23 sec and gas injection was terminated 92 sec into run 105, it is evident that residual temperature differences had essentially disappeared 18 min after gas injection was terminated.

Results and Conclusions

The effect of inert-gas injection on steady-state nonboiling conditions downstream of a central blockage in THORS bundle 3B is summarized as follows:

No general correlation could be established between blockage wake temperature increase due to gas injection and void fraction, heater power, and flow from the nine test runs analyzed.

Of the nine test runs (where void fractions were between 0.00009 and 0.00354), only one (run 104) showed peak thermocouple temperature increases due to gas injection in excess of 17°C (30°F). The test conditions for run 104 were: α = 0.00065, test-section flow = 1.23 liters/sec (19.5 gpm), heater power = 20 kW/m (6.1 kW/ft), and inlet temperature = 322°C (611°F);

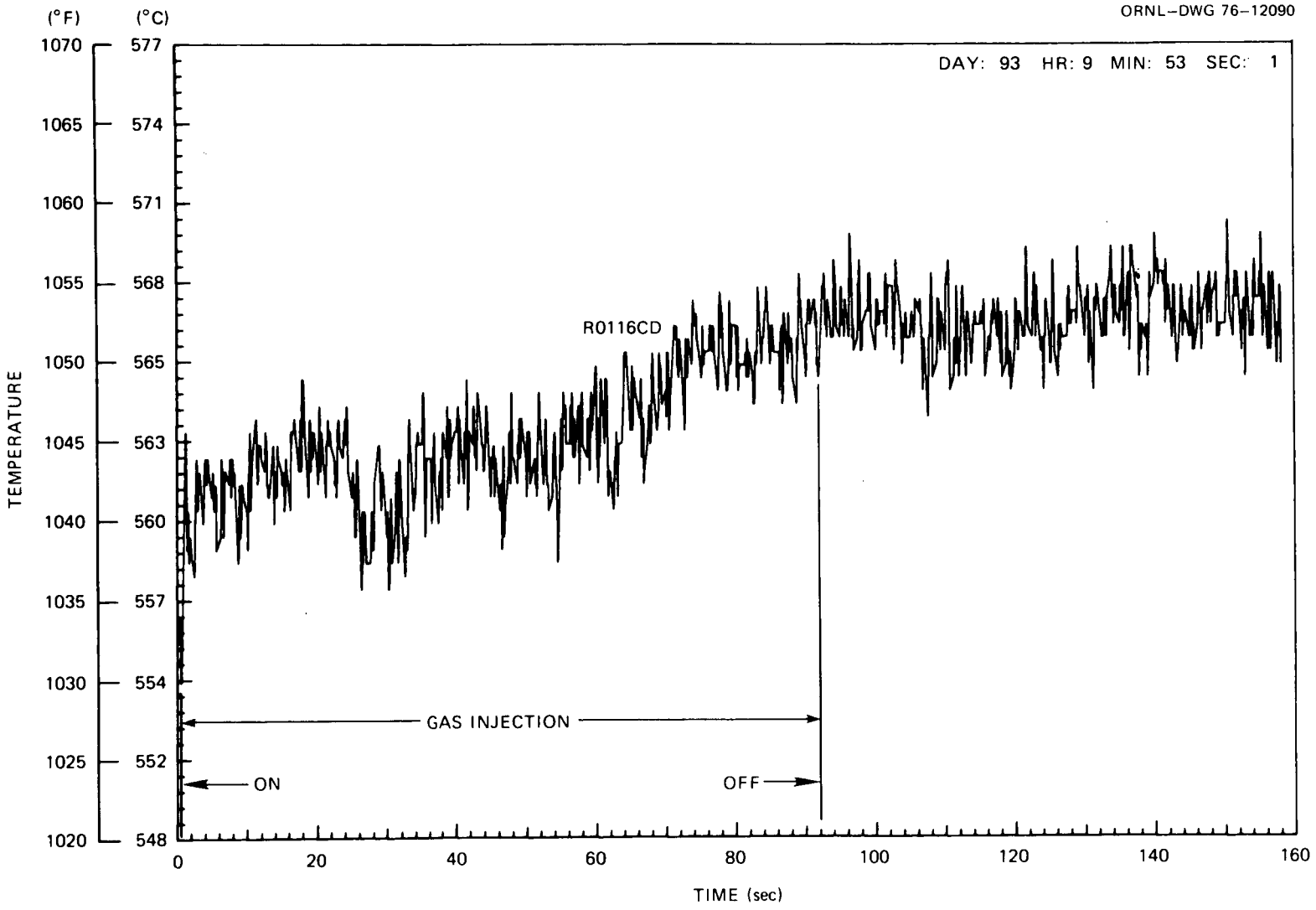

Fig. 24. Response of internal heater thermocouple R0116CD during test series 8, test 2, run 105, α = 0.00022. R0116CD is located on heater 1, 15.63 in. downstream from the start of the heated section and 0.63 in. downstream of the blockage (see Fig. 10).

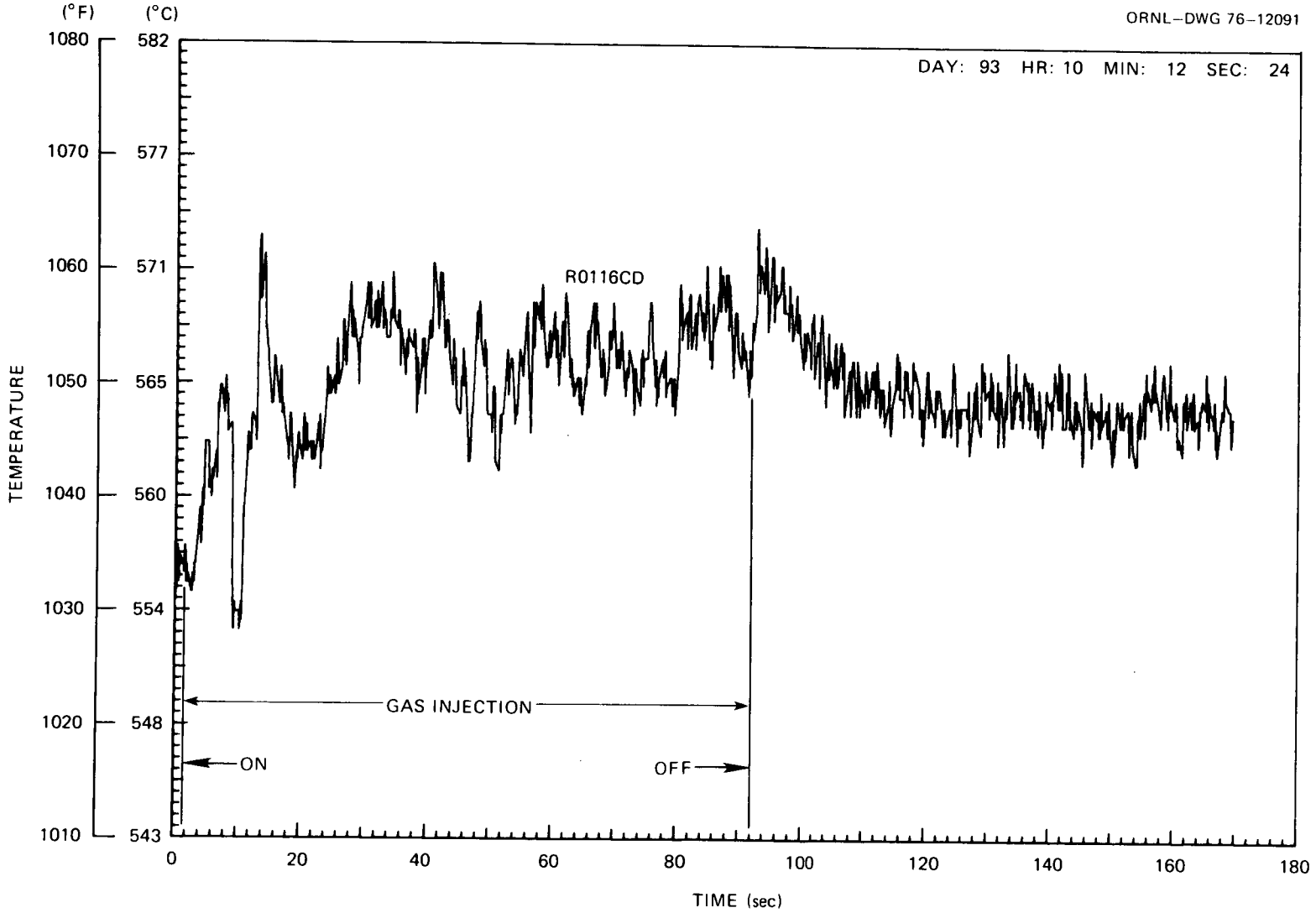

Fig. 25. Response of internal heater thermocouple R0116CD during test series 8, test 2, run 106, α = 0.00087. R0116CD is located on heater 1, 15.63 in. downstream from the start of the heated section and 0.63 in. downstream of the blockage (see Fig. 10).

the peak temperature increase due to gas injection measured during this run was 39°C (70°F) and occurred in the blockage wake at 16 mm (0.63 in.) downstream of the blockage.

The largest average temperature increase during an entire period of gas injection (61 sec) was 35°C (63°F); it occurred in run 104 at 16 mm (0.63 in.) downstream of the blockage.

The maximum combined increase of sodium temperature (over the calculated sodium temperature in an unblocked 19-rod bundle) due to both gas injection (α = 0.00065) and the 6-channel central blockage was estimated to be no more than 160°C (290°F). Such a maximum temperature increase, however, is only valid for the nine unique combinations of void fraction, flow, and heater power used in the bundle 3B experiments.

Residual temperature increases after gas injection give evidence that gas downstream of the bundle 3B blockage was completely removed from the wake between 3 and 18 min after a 90-sec period of gas injection for the void fractions investigated.

OVERALL CONCLUSIONS ON RESULTS OF BUNDLE 3B TESTS

Although bundle 3B was not specifically designed for boiling tests, it is possible to show from the data that, without argon gas injection, the local boiling zone in a 6-channel blockage wake does not radially propagate into the unblocked channels during as much as 27 sec of quasi-steady-state boiling. Indications are that argon gas injection during quasi-steady-state boiling does influence the extent of the local boiling zone by radially propagating it into some unblocked channels but not across the entire bundle cross section. It was shown that the sodium bulk temperature in the free stream adjacent to the blockage wake (calculated from the power-to-flow ratio) strongly influences the radial extent of any propagation, since it governs the condensation capability of sodium vapor. Therefore, since it is expected that the sodium bulk temperature in a 217-pin LMFBR subassembly is well below the sodium saturation temperature, an idealized extrapolation of bundle 3B results shows that the vapor-condensing capability in an LMFBR subassembly makes any radial propagation of the local boiling zone unlikely.

Axial propagation of the local boiling zone could not be investigated with bundle 3B because of several nonprototypicalities in the THORS test facility; facility modifications are planned to eliminate these dynamic non-prototypicalities.

Argon gas injection at several different void fractions during single-phase steady-state tests does not raise the temperature in the blockage wake by more than 40°C (70°F). Considering that the maximum temperature increase caused by a 6-channel blockage alone was show to be no more than 120°C (220°F) in previous tests with the same rod bundle, the additional temperature increase due to gas injection (at the void fractions investigated) does not appear to be excessive from the standpoint of initiating local sodium boiling in the blockage wake.

REFERENCES

1. A. G. Grindell and R. E. MacPherson, *Final Systems Design Description of the Fuel Failure Mockup of the LMFBR*, ORNL/TM-3656 (September 1972).

2. M. H. Fontana et al., *Temperature Distribution in a 19-Rod Simulated LMFBR Fuel Assembly in a Scalloped Duct (Fuel Failure Mockup Bundle 1B) — Record of Experimental Data*, ORNL/TM-4939 (November 1975).

3. M. H. Fontana et al., *Temperature Distribution in a 19-Rod Simulated LMFBR Fuel Assembly in a Hexagonal Duct (Fuel Failure Mockup Bundle 2A — Record of Experimental Data*, ORNL/TM-4113 (September 1973).

4. M. H. Fontana et al., *Temperature Distribution in a 19-Rod Simulated LMFBR Fuel Rod Bundle with Inlet Blockages (FFM Bundle 2B)*, ORNL/TM-4367 (January 1974).

5. M. H. Fontana et al., *Temperature Distribution in a 19-Rod Simulated LMFBR Fuel Assembly with a Six-Channel Internal Blockage (Fuel Failure Mockup Bundle 3A) — Record of Experimental Data*, ORNL/TM-5101 (March 1976).

6. M. H. Fontana et al., *Temperature Distribution in a 19-Rod Simulated LMFBR Fuel Assembly with an Edge Blockage (Out-of-Reactor Test for ANL FEFP P1 Experiment) — Record of Experimental Data for Fuel Failure Mockup Bundle 5A*, ORNL/TM-4633 (November 1974).

7. M. H. Fontana et al., *Fuel Failure Mockup Bundles 5B and 5C — Record of Experimental Data*, ORNL/TM-5003 (January 1976).

8. J. L. Wantland et al., *Fuel Failure Mockup Bundle 5D — Record of Experimental Data*, ORNL/TM-5580 (February 1977).

9. *Job Specification, Reactor Division, Oak Ridge National Laboratory, Heaters for FFM Bundle 3*, ORNL Specification JS-174-246 (Aug. 26, 1971).

10. D. L. Clark, "Adapting Commercial Heaters to Simulate LMFBR Fuel Rods in Sodium," *Trans. Amer. Nucl. Soc.* 13(2), 817 (1970).

11. R. E. MacPherson and D. L. Clark, "High Performance Electric Heaters for LMFBR Fuel Pin Simulation," *Trans. Amer. Nucl. Soc.* 15(1), 366–67 (1972).

12. M. H. Fontana and J. L. Wantland, *LMFBR Safety and Core Systems Programs Progress Report January–March 1975*, ORNL/TM-4980.

13. J. L. Wantland et al., *Sodium Boiling Tests in a 19-Rod Bundle with a Central Blockage — Record of Experimental Data for Fuel Failure Mockup Bundle 3B*, ORNL/TM-5458 (October 1976).

14. J. T. Han et al., "Thermal-Hydraulic Correlations of a Six-Channel Blockage in a Sodium-Cooled Simulated LMFBR Fuel Assembly," presented at the International Meeting on Fast Reactor Safety, Chicago, Illinois, October 5–8, 1976, CONF-761001 (to be published).

15. M. H. Fontana et al., *Effect of Partial Blockages in Simulated LMFBR Fuel Assemblies*, ORNL/TM-4324 (December 1973).

ORNL/TM-5862
Dist. Category UC-79,
-79e, -79p

Internal Distribution

1. A. H. Anderson
2. S. Baron
3. N. E. Clapp
4. C. W. Collins
5. W. E. Cooper
6. W. B. Cottrell
7. F. L. Culler, Jr.
8. J. F. Dearing
9. G. G. Fee
10-19. M. H. Fontana
20. D. N. Fry
21. P. W. Garrison
22. P. A. Gnadt
23. M. J. Goglia
24. A. G. Grindell
25. J. T. Han
26-31. N. Hanus
32. W. O. Harms
33. J. F. Harvey
34. R. A. Hedrick
35. H. W. Hoffman
36. T. L. Hudson
37. T. S. Kress
38. W. H. Leavell
39. M. Levenson
40. R. E. MacPherson
41. C. D. Martin
42. M. V. Mathes
43. R. W. McCulloch
44. R. L. Moore
45. B. H. Montgomery
46. R. H. Morris
47. L. C. Oakes
48. L. F. Parsly
49. R. J. Ribando
50. J. L. Redford
51. M. R. Sheldon
52. W. H. Sides
53. M. J. Skinner
54. C. M. Smith
55. I. Spiewak
56. D. G. Thomas
57. R. H. Thornton
58. D. B. Trauger
59. J. L. Wantland
60. G. D. Whitman
61. W. J. Wilcox
62. R. Saxe (Consultant)
63-64. Central Research Library
65. Y-12 Document Reference Section
66-67. Laboratory Records Department
68. Laboratory Records (RC)

External Distribution

69. Assistant Administrator, Nuclear Energy, ERDA, Washington, D.C. 20545
70-71. Director, Division of Reactor Development and Demonstration, U.S. Energy Research and Development Administration, Washington, D.C. 20545
72. Director, Reactor Division, ERDA, Oak Ridge Operations Office
73. Research and Technical Support Division, ERDA, Oak Ridge Operations Office
74-312. For distribution as shown in TID-4500 under categories UC-79, -79e, and -79p

☆ U.S. GOVERNMENT PRINTING OFFICE: 1976-748-189/60